7

NEUTRINO OSCILLATIONS IN VACUUM

> The ability to perceive or think differently is more important than the knowledge gained.
> **David Bohm**

Neutrino oscillation is a quantum mechanical phenomenon proposed in the late 1950s by Pontecorvo [880, 881] in analogy with K^0-$\bar{K}^0$ oscillations. The oscillations are generated by the interference of different massive neutrinos, which are produced and detected coherently because of their very small mass differences.

Since in the late 1950s only one *active* neutrino was known, the electron neutrino, in order to discuss neutrino oscillations, Pontecorvo invented the concept of a *sterile* neutrino [883], which is a neutral fermion which does not take part in weak interactions. The muon neutrino was discovered in 1962 in the Brookhaven experiment of Lederman, Schwartz, Steinberger, *et al.* [348], who followed up a proposal made by Pontecorvo in 1959 [882]. Since then, it became clear that oscillations between different active neutrino flavors are possible if neutrinos are massive and mixed. In 1962 Maki, Nakagawa, and Sakata [766] considered for the first time a model with the mixing of different neutrino flavors. In 1967 Pontecorvo [883] predicted the Solar Neutrino Problem as a consequence of $\nu_e \to \nu_\mu$ (or $\nu_e \to \nu_{\rm sterile}$) transitions even before the first measurement of the solar electron neutrino flux in the Homestake experiment [323], and in 1969 Gribov and Pontecorvo discussed solar neutrino oscillations due to neutrino mixing [567].

However, in the above and other papers, the probability of neutrino oscillations was not calculated in a rigorous way, but simply estimated on the basis of the analogy with kaon oscillations. As a result, the phase of the oscillations was correct within a factor of two.

The standard theory of neutrino oscillations in the plane-wave approximation was developed in 1975–76 by Eliezer and Swift [404], Fritzsch and Minkowski [466], Bilenky and Pontecorvo [236, 239], and elegantly reviewed by Bilenky and Pontecorvo in Ref. [237].

In this chapter, we review the standard plane-wave derivation of the neutrino oscillation probability in section 7.1. In the following sections, we discuss the main phenomenological aspects of neutrino oscillations in vacuum.

An important feature necessary for the derivation of a simple and general expression for the probability of neutrino oscillations is the fact that neutrinos in oscillation experiments are ultrarelativistic, since neutrino masses are smaller than about one eV (see chapter 14) and only neutrinos with energy larger than about 100 keV can be detected. Neutrinos are detected in:

1. Charged-current or neutral-current weak scattering processes which have an energy threshold given in eqn (5.37). As shown in Table 5.2 (page 143), current experimental thresholds are always larger than some fraction of an MeV. The lowest threshold reached so far is that of the first reaction in Table 5.2, $\nu_e + {}^{71}\mathrm{Ga} \to {}^{71}\mathrm{Ge} + e^-$, which is used in gallium solar neutrino experiments (see section 10.5).
2. The elastic scattering process $\nu + e^- \to \nu + e^-$, whose cross-section is proportional to the neutrino energy ($\sigma(E_\nu) \sim \sigma_0 E_\nu / m_e$, with $\sigma_0 \sim 10^{-44}\,\mathrm{cm}^2$). An energy threshold of some MeV's is needed in order to have a signal above the background. For example, $E_\nu^{\mathrm{th}} \simeq 5\,\mathrm{MeV}$ in the Super-Kamiokande [472] solar neutrino experiment.

Neutrinos ν_α with flavor $\alpha = e, \mu, \tau$ are produced[35] in charged-current (CC) weak interaction processes from a charged lepton ℓ_α^- (i.e. $\ell_\alpha^- \to \nu_\alpha$ transitions) or together with a charged antilepton ℓ_α^+ (i.e. creation of a ℓ_α^+ ν_α pair). These processes are generated by the charged-current leptonic interaction Lagrangian (see eqns (3.76) and (3.77))

$$\mathscr{L}_{\mathrm{I,L}}^{(\mathrm{CC})} = -\frac{g}{2\sqrt{2}} \left(j_{W,\mathrm{L}}^{\rho} W_\rho + j_{W,\mathrm{L}}^{\rho\dagger} W_\rho^\dagger \right) , \tag{7.1}$$

where $j_{W,\mathrm{L}}^{\rho}$ is the leptonic charged current

$$j_{W,\mathrm{L}}^{\rho} = 2 \sum_{\alpha=e,\mu,\tau} \overline{\nu_{\alpha L}}\, \gamma^\rho\, \ell_{\alpha L} = 2 \sum_{\alpha=e,\mu,\tau} \sum_k U_{\alpha k}^*\, \overline{\nu_{kL}}\, \gamma^\rho\, \ell_{\alpha L} , \tag{7.2}$$

which is valid both in the case of Dirac (see eqns (6.14) and (6.187)) or Majorana massive neutrinos (see eqn (6.184)). In the case of Dirac neutrinos, the Fourier expansion of the field operator $\overline{\nu_k}$ is (see eqn (2.139))

$$\overline{\nu_{kL}}(x) = \int \frac{\mathrm{d}^3 p}{(2\pi)^3\, 2E} \sum_{h=\pm 1} \left[a_{\nu_k}^{(h)\dagger}(p)\, \overline{u_{\nu_k L}^{(h)}}(p)\, e^{-ip\cdot x} + b_{\nu_k}^{(h)}(p)\, \overline{v_{\nu_k L}^{(h)}}(p)\, e^{ip\cdot x} \right] . \tag{7.3}$$

Hence, the leptonic charged current in eqn (7.2) contains creation operators $a_{\nu_k}^{(h)\dagger}(p)$ of neutrinos with mass m_k and, through the charged lepton field ℓ_α, it contains destruction operators of ℓ_α^- and creation operators of ℓ_α^+, which lead to the generation of $\ell_\alpha^- \to \nu_k$ transitions or ℓ_α^+ ν_k pair creation.

In the case of Majorana neutrinos, we have $b_{\nu_k}^{(h)}(p) = a_{\nu_k}^{(h)}(p)$ (see eqn (6.99)). Hence, creation operators $a_{\nu_k}^{(h)\dagger}(p)$ of neutrinos with mass m_k are present both in

[35] Neutrinos can also be produced in the neutral-current (NC) weak interaction process $Z \to \nu\bar{\nu}$, generated by the interaction Lagrangian in eqn (3.90). The Z can be either real (Z-decay) or virtual (for example in $e^- e^+ \to \nu\bar{\nu}$). In this case, the neutrinos do not have a definite flavor. However, the produced neutrinos are active and can oscillate into sterile neutrinos if light sterile neutrinos exist. These oscillations could be observed by measuring the disappearance of active neutrinos. The theory of active–sterile oscillations can be obtained by straightforward modifications to the theory of flavor oscillations discussed in this chapter.

$j^{\rho}_{W,\mathrm{L}}$ and $j^{\rho\dagger}_{W,\mathrm{L}}$. However, $j^{\rho\dagger}_{W,\mathrm{L}}$ does not contribute to $\ell^-_\alpha \to \nu_k$ transitions or $\ell^+_\alpha\ \nu_k$ pair creation because it contains the charged lepton field in the adjoint form $\overline{\ell_\alpha}$, which does not contain destruction operators of ℓ^-_α and creation operators of ℓ^+_α (it contains creation operators of ℓ^-_α and destruction operators of ℓ^+_α).

The leptonic charged current in eqn (7.2) generates a superposition of massive neutrinos if the energies and momenta of the particles which participate in the neutrino production process are not measured with a degree of accuracy which would allow the determination, through energy–momentum conservation, of the massive neutrino which is emitted. This is characteristic of neutrino oscillation experiments, in which a flavor neutrino ν_α is a superposition of massive neutrinos ν_k with weights proportional to $U^*_{\alpha k}$.

7.1 Standard Derivation of the Neutrino Oscillation Probability

In the standard theory of neutrino oscillations [404, 466, 236, 239, 237] a neutrino with flavor α and momentum $\vec{p}$, created in a charged-current weak interaction process from a charged lepton ℓ^-_α or together with a charged antilepton ℓ^+_α, is described by the flavor state

$$|\nu_\alpha\rangle = \sum_k U^*_{\alpha k}\,|\nu_k\rangle \qquad (\alpha = e, \mu, \tau)\,. \tag{7.4}$$

The presence of the weight $U^*_{\alpha k}$ of the $|\nu_k\rangle$ in the flavor state $|\nu_\alpha\rangle$ is due to the decomposition in eqn (7.2) of the leptonic charged current $j^{\rho}_{W,\mathrm{L}}$ in terms of the massive neutrino contributions, which contain the creation operators of massive neutrinos. As we will see in subsection 8.1.1, additional coefficients due to the effect of the difference of the neutrino masses on the interaction process are negligible for neutrino oscillations.

For simplicity, we consider a finite normalization volume V, according to the method discussed in section 2.13, in order to have orthonormal massive neutrino states:

$$\langle \nu_k | \nu_j \rangle = \delta_{kj}\,. \tag{7.5}$$

The unitarity of the mixing matrix implies that also the flavor states are orthonormal:

$$\langle \nu_\alpha | \nu_\beta \rangle = \delta_{\alpha\beta}\,. \tag{7.6}$$

In eqn (7.4) we have not limited the number of massive neutrinos. Since it is known that the number of active flavor neutrinos is three, corresponding to ν_e, ν_μ, ν_τ, the number of massive neutrinos must be equal to or greater than three. If the number of massive neutrinos is greater than three, the additional neutrinos in the flavor basis are sterile, i.e. they do not participate in weak interactions (since neutrinos are electrically neutral, sterile neutrinos interact with ordinary matter only through gravitational interactions or exotic interactions beyond those in the SM). Transitions of active flavor neutrinos into sterile ones can be observed only through the disappearance of active neutrinos.

The massive neutrino states $|\nu_k\rangle$ are eigenstates of the Hamiltonian,

$$\mathscr{H}|\nu_k\rangle = E_k|\nu_k\rangle\,, \tag{7.7}$$

with energy eigenvalues

$$E_k = \sqrt{\vec{p}^{\,2} + m_k^2}\,. \tag{7.8}$$

The Schrödinger equation

$$i\,\frac{\mathrm{d}}{\mathrm{d}t}\,|\nu_k(t)\rangle = \mathscr{H}\,|\nu_k(t)\rangle \tag{7.9}$$

implies that the massive neutrino states evolve in time as plane waves:

$$|\nu_k(t)\rangle = e^{-iE_k t}\,|\nu_k\rangle\,. \tag{7.10}$$

Let us consider now a flavor state $|\nu_\alpha(t)\rangle$ which describes a neutrino created with a definite flavor α at time $t = 0$. From eqns (7.4) and (7.10), the time evolution of this state is given by

$$|\nu_\alpha(t)\rangle = \sum_k U^*_{\alpha k}\, e^{-iE_k t}\,|\nu_k\rangle\,, \tag{7.11}$$

such that

$$|\nu_\alpha(t=0)\rangle = |\nu_\alpha\rangle\,. \tag{7.12}$$

Using the unitarity relation

$$U^\dagger\, U = \mathbf{1} \quad\Longleftrightarrow\quad \sum_\alpha U^*_{\alpha k}\, U_{\alpha j} = \delta_{jk}\,, \tag{7.13}$$

the massive states can be expressed in terms of flavor states inverting eqn (7.4):

$$|\nu_k\rangle = \sum_\alpha U_{\alpha k}\,|\nu_\alpha\rangle\,. \tag{7.14}$$

Substituting eqn (7.14) into eqn (7.11), we obtain

$$|\nu_\alpha(t)\rangle = \sum_{\beta=e,\mu,\tau}\left(\sum_k U^*_{\alpha k}\, e^{-iE_k t}\, U_{\beta k}\right)|\nu_\beta\rangle\,. \tag{7.15}$$

Hence, the superposition of massive neutrino states $|\nu_\alpha(t)\rangle$, which is the pure flavor state given in eqn (7.4) at $t = 0$, becomes a superposition of different flavor states at $t > 0$ (if the mixing matrix U is not diagonal, i.e. neutrinos are mixed). The

coefficient of $|\nu_\beta\rangle$,

$$A_{\nu_\alpha \to \nu_\beta}(t) \equiv \langle \nu_\beta | \nu_\alpha(t) \rangle = \sum_k U^*_{\alpha k}\, U_{\beta k}\, e^{-iE_k t}\,, \tag{7.16}$$

is the amplitude of $\nu_\alpha \to \nu_\beta$ transitions as a function of time. The transition probability is, then, given by

$$P_{\nu_\alpha \to \nu_\beta}(t) = \left| A_{\nu_\alpha \to \nu_\beta}(t) \right|^2 = \sum_{k,j} U^*_{\alpha k}\, U_{\beta k}\, U_{\alpha j}\, U^*_{\beta j}\, e^{-i(E_k - E_j)t}\,. \tag{7.17}$$

For ultrarelativistic neutrinos, the dispersion relation in eqn (7.8) can be approximated by

$$E_k \simeq E + \frac{m_k^2}{2E}\,. \tag{7.18}$$

In this case,

$$E_k - E_j \simeq \frac{\Delta m^2_{kj}}{2E}\,, \tag{7.19}$$

where Δm^2_{kj} is the squared-mass difference

$$\Delta m^2_{kj} \equiv m^2_k - m^2_j\,, \tag{7.20}$$

and

$$E = |\vec{p}| \tag{7.21}$$

is the neutrino energy, neglecting the mass contribution. Therefore, the transition probability in eqn (7.17) can be approximated by

$$P_{\nu_\alpha \to \nu_\beta}(t) = \sum_{k,j} U^*_{\alpha k} U_{\beta k} U_{\alpha j} U^*_{\beta j} \exp\left(-i \frac{\Delta m^2_{kj} t}{2E} \right)\,. \tag{7.22}$$

The final step in the standard derivation of the neutrino oscillation probability is based on the fact that, in neutrino oscillation experiments, the propagation time t is not measured. What is known is the distance L between the source and the detector. Since ultrarelativistic neutrinos propagate almost at the speed of light, it is possible to approximate $t = L$, leading to

$$P_{\nu_\alpha \to \nu_\beta}(L, E) = \sum_{k,j} U^*_{\alpha k}\, U_{\beta k}\, U_{\alpha j}\, U^*_{\beta j}\, \exp\left(-i\, \frac{\Delta m^2_{kj} L}{2E} \right)\,. \tag{7.23}$$

This expression shows that the source–detector distance L and the neutrino energy E are the quantities depending on the experiment which determine the phases of neutrino oscillations

$$\Phi_{kj} = -\frac{\Delta m^2_{kj}\, L}{2\, E}\,. \tag{7.24}$$

Of course, the phases are determined also by the squared-mass differences Δm^2_{kj}, which are physical constants. The amplitude of the oscillations is specified only

by the elements of the mixing matrix U, which are constants of nature. Therefore measurements of neutrino oscillations allow one to shed some light on the values of the squared-mass differences Δm^2_{kj} and the elements of the mixing matrix U.

Although positive measurements of neutrino oscillations imply massive neutrinos, they yield precise information only on the values of the squared-mass differences Δm^2_{kj}, but not on the absolute values of neutrino masses, except that obviously m^2_k or m^2_j must be larger than $|\Delta m^2_{kj}|$.

The oscillation probability in eqn (7.23) depends on the elements of the mixing matrix U through the quartic products

$$U^*_{\alpha k}\, U_{\beta k}\, U_{\alpha j}\, U^*_{\beta j}\,, \tag{7.25}$$

which do not depend on the specific parameterization of the mixing matrix and on the choice of phases. In fact, the quartic products in eqn (7.25) are invariant under the rephasing transformation

$$U_{\alpha k} \to e^{i\psi_\alpha}\, U_{\alpha k}\, e^{i\phi_k}\,. \tag{7.26}$$

Hence, the quartic products eqn (7.25) do not depend on the phases that can be factorized on the left or on the right of the mixing matrix. This corresponds to a rephasing of the charged lepton and neutrino fields.

As we have discussed in section 6.3, in the case of Majorana neutrinos the three-neutrino mixing matrix contains, in addition to the Dirac phase analogous to that in the CKM mixing matrix of quarks, two Majorana phases which appear in a diagonal matrix at the right of the mixing matrix. In other words, as shown in eqn (6.189), we can write

$$U_{\alpha k} = U^{\rm D}_{\alpha k}\, e^{i\lambda_k}\,. \tag{7.27}$$

The rephasing invariants in eqn (7.25) are free from the Majorana phases. This means that the Majorana phases cannot be measured in neutrino oscillation experiments (see section 9.2 for the proof that this statement holds also in the case of neutrino oscillations in matter). This statement holds in general for any number of generations: neutrino oscillations are independent of the Majorana phases, which are always factorized in a diagonal matrix on the right of the mixing matrix. In particular, CP and T violations in neutrino oscillations, discussed in sections 7.3.2 and 7.3.3, depend only on the Dirac phases.

It is clear that transitions among different flavors manifest for $L > 0$, because the unitarity relation

$$U\,U^\dagger = \mathbf{1} \quad \Longleftrightarrow \quad \sum_k U_{\alpha k}\, U^*_{\beta k} = \delta_{\alpha\beta} \tag{7.28}$$

implies that

$$P_{\nu_\alpha \to \nu_\beta}(L = 0, E) = \delta_{\alpha\beta}\,. \tag{7.29}$$

Sometimes it is convenient to write the probability in eqn (7.23) as

$$P_{\nu_\alpha \to \nu_\beta}(L, E) = \sum_k |U_{\alpha k}|^2\, |U_{\beta k}|^2 + 2\Re\mathfrak{e} \sum_{k>j} U^*_{\alpha k}\, U_{\beta k}\, U_{\alpha j}\, U^*_{\beta j}\, \exp\left(-2\pi i\, \frac{L}{L^{\rm osc}_{kj}}\right)\,, \tag{7.30}$$

in which we have separated a constant term from the oscillating term and we have defined the oscillation lengths

$$L_{kj}^{\rm osc} = \frac{4\pi E}{\Delta m_{kj}^2} \,. \tag{7.31}$$

The oscillation length $L_{kj}^{\rm osc}$ is the distance at which the phase generated by Δm_{kj}^2 becomes equal to 2π.

The oscillating term in eqn (7.30) is produced by the interference of the different massive neutrino components of the state in eqn (7.11). Therefore, its existence depends on the coherence of the massive neutrino components. If, for some reason, different massive neutrinos are produced or detected in an incoherent way, as discussed in section 8.2.2, the probability of $\nu_\alpha \to \nu_\beta$ reduces to the constant term in eqn (7.30), as can also be seen by calculating the incoherent transition probability

$$P_{\nu_\alpha \to \nu_\beta}^{\rm incoherent} = \sum_k \left| \langle \nu_\beta | \nu_k \rangle \, e^{-iE_k t} \, \langle \nu_k | \nu_\alpha \rangle \right|^2 = \sum_k |U_{\alpha k}|^2 \, |U_{\beta k}|^2 \,. \tag{7.32}$$

As discussed in section 7.6, the incoherent average of the oscillation probability in eqn (7.30) over the energy resolution of the detector or over the uncertainty of the distance L can also lead to an effectively constant measurable probability which has the same value as the incoherent transition probability in eqn (7.32):

$$\langle P_{\nu_\alpha \to \nu_\beta} \rangle = \sum_k |U_{\alpha k}|^2 \, |U_{\beta k}|^2 \,. \tag{7.33}$$

This result follows simply from the fact that the average of the exponential functions in eqn (7.30) is zero.

The oscillation probability in eqn (7.23) satisfies the two rules of the conservation of probability which are consequences of the unitary evolution of the states:

1. The sum of the probabilities of transition from a flavor neutrino ν_α to all flavor neutrinos ν_β (including $\alpha = \beta$) is equal to unity:

$$\sum_\beta P_{\nu_\alpha \to \nu_\beta}(L, E) = 1 \,. \tag{7.34}$$

2. The sum of the probabilities of transition from any flavor neutrino ν_α (including $\alpha = \beta$) to a flavor neutrino ν_β is equal to unity:

$$\sum_\alpha P_{\nu_\alpha \to \nu_\beta}(L, E) = 1 \,. \tag{7.35}$$

These sum rules can be derived from eqn (7.23) by using the unitarity relations in eqns (7.13) and (7.28).

Another useful way to write the oscillation probability in eqn (7.23) is to separate the real and imaginary parts of $U_{\beta k} \, U_{\alpha k}^* \, U_{\beta j}^* \, U_{\alpha j}$. From the square of the unitarity

relation in eqn (7.28), we obtain

$$\sum_k |U_{\alpha k}|^2 \, |U_{\beta k}|^2 = \delta_{\alpha\beta} - 2 \sum_{k>j} \Re\mathfrak{e}\big[U^*_{\alpha k} \, U_{\beta k} \, U_{\alpha j} \, U^*_{\beta j}\big] \ , \tag{7.36}$$

which allows one to write the oscillation probability as

$$\begin{aligned} P_{\nu_\alpha \to \nu_\beta}(L,E) = \delta_{\alpha\beta} &- 2 \sum_{k>j} \Re\mathfrak{e}\big[U^*_{\alpha k} \, U_{\beta k} \, U_{\alpha j} \, U^*_{\beta j}\big] \left[1 - \cos\left(\frac{\Delta m^2_{kj} L}{2E}\right)\right] \\ &+ 2 \sum_{k>j} \Im\mathfrak{m}\big[U^*_{\alpha k} \, U_{\beta k} \, U_{\alpha j} \, U^*_{\beta j}\big] \, \sin\left(\frac{\Delta m^2_{kj} L}{2E}\right) \ , \end{aligned} \tag{7.37}$$

or in the form

$$\begin{aligned} P_{\nu_\alpha \to \nu_\beta}(L,E) = \delta_{\alpha\beta} &- 4 \sum_{k>j} \Re\mathfrak{e}\big[U^*_{\alpha k} \, U_{\beta k} \, U_{\alpha j} \, U^*_{\beta j}\big] \, \sin^2\left(\frac{\Delta m^2_{kj} L}{4E}\right) \\ &+ 2 \sum_{k>j} \Im\mathfrak{m}\big[U^*_{\alpha k} \, U_{\beta k} \, U_{\alpha j} \, U^*_{\beta j}\big] \, \sin\left(\frac{\Delta m^2_{kj} L}{2E}\right) \ . \end{aligned} \tag{7.38}$$

The oscillation probabilities of the channels with $\alpha \neq \beta$ are usually called *transition probabilities*, whereas the oscillation probabilities of the channels with $\alpha = \beta$ are usually called *survival probabilities*. Since, in the case of the survival probabilities, the quartic products in eqn (7.25) are real and equal to $|U_{\alpha k}|^2 |U_{\alpha j}|^2$, the survival probabilities can be written in the simple form

$$P_{\nu_\alpha \to \nu_\alpha}(L,E) = 1 - 4 \sum_{k>j} |U_{\alpha k}|^2 \, |U_{\alpha j}|^2 \, \sin^2\left(\frac{\Delta m^2_{kj} L}{4E}\right) \ . \tag{7.39}$$

It is interesting to see for which values of $|U_{\alpha k}|^2$ and $|U_{\beta k}|^2$ with $\alpha \neq \beta$, the average transition probability in eqn (7.33) has its maximum. Since the values of $|U_{\alpha k}|^2$ and $|U_{\beta k}|^2$ are subject to the unitarity constraints

$$\sum_k |U_{\alpha k}|^2 = 1 \qquad \text{and} \qquad \sum_k |U_{\beta k}|^2 = 1 \, , \tag{7.40}$$

we can use the method of the Lagrange multipliers and calculate the stationary point of

$$f(|U_{\alpha k}|^2, |U_{\beta k}|^2) = \sum_k |U_{\alpha k}|^2 \, |U_{\beta k}|^2 - a \left(1 - \sum_k |U_{\alpha k}|^2\right) - b \left(1 - \sum_k |U_{\beta k}|^2\right) \ , \tag{7.41}$$

where a and b are the Lagrange multipliers. The stationary point is given by

$$0 = \frac{\mathrm{d}f}{\mathrm{d}|U_{\alpha k}|^2} = |U_{\beta k}|^2 + a \, , \qquad 0 = \frac{\mathrm{d}f}{\mathrm{d}|U_{\beta k}|^2} = |U_{\alpha k}|^2 + b \, . \tag{7.42}$$

Hence, for fixed $\alpha \neq \beta$ and different values of k, all $|U_{\alpha k}|^2$ are the same and all $|U_{\beta k}|^2$ are the same too. From the constraints in eqn (7.40) we find the solution

$$|U_{\alpha k}|^2 = |U_{\beta k}|^2 = \frac{1}{N} \quad \text{for all} \quad k \quad \Longrightarrow \quad \langle P_{\nu_\alpha \to \nu_\beta} \rangle_{\max} = \frac{1}{N} \qquad (\alpha \neq \beta)\,, \tag{7.43}$$

where N is the number of massive neutrinos. Similarly, one can show that in the case of the survival probabilities

$$|U_{\alpha k}|^2 = \frac{1}{N} \quad \text{for all} \quad k \quad \Longrightarrow \quad \langle P_{\nu_\alpha \to \nu_\alpha} \rangle_{\min} = \frac{1}{N}\,. \tag{7.44}$$

Therefore, the case in which all the elements of the $N \times N$ mixing matrix have the same absolute value, usually called *N-maximal mixing*, corresponds to minimal average survival probability equal to $1/N$ and maximal average transition probability equal to $1/N$ in each possible channel, in such a way that the sum of the average survival probability and all the average transition probabilities add up correctly to unity.

Let us finally summarize and comment on the three main assumptions adopted in the standard derivation of the neutrino oscillation probability.

(A1) Neutrinos produced or detected in CC weak interaction processes are described by the flavor states in eqn (7.4). As we will see in subsection 8.1.1 the states which describe flavor neutrinos can be derived in the framework of quantum field theory. We will show that these flavor states reduce to the standard ones in eqn (7.4) in the case of experiments which are not sensitive to the differences of the contributions of the different neutrino masses to the production and detection processes. This is the case for all neutrino oscillation experiments.

(A2) Flavor neutrinos have a definite momentum $\vec{p}$, i.e. all the massive neutrino components have the same momentum. This is sometimes called the *equal momentum assumption*. It may have been motivated by the fact that all the components propagate in the same direction from source to detector. However, there is no justification for this assumption and we will see in section 8.4.3 that it is, in fact, unrealistic. Luckily, however, the equal momentum assumption is irrelevant in the derivation of the oscillation probability, as will be seen in section 8.1.2.

(A3) The propagation time t is equal to the distance L traveled by the neutrino between production and detection. It is sometimes called the *light-ray approximation*. This assumption is unjustified in a plane-wave treatment of oscillations, because plane waves extend with the same amplitude over the whole space-time. However, in quantum theory, localized particles are described by wave packets. As will be discussed in section 8.2, in the case of neutrino oscillation experiments, neutrinos are described by wave packets [660, 533, 528, 225, 523, 526] that are localized in the production process at the production time and propagate between the production and the detection processes with a group velocity close to the velocity of light, justifying the approximation $t = L$.

From eqn (2.472), the group velocity $\vec{v}_k$ of an ultrarelativistic neutrino with mass m_k, average wave packet momentum $\vec{p}_k$ and average wave packet energy

E_k is given by

$$\vec{v}_k = \frac{\vec{p}_k}{E_k} \simeq \frac{\vec{p}_k}{|\vec{p}_k|} \left(1 - \frac{m_k^2}{2E^2}\right) . \tag{7.45}$$

Since, in oscillation experiments, all massive neutrinos are produced and detected in the same localized processes, their group velocities have the same direction. However, since the absolute value of the group velocities of different massive neutrinos are different, there is a separation of the wave packets which increases with the distance from the production process. Nevertheless, different massive neutrino wave packets can contribute coherently to the detection process if they overlap in a sufficient way.

If the massive neutrinos are ultrarelativistic and contribute coherently to the detection process, their wave packets overlap with the detection process for an interval of time $[t - \Delta t\,,\, t + \Delta t]$, with

$$t = \frac{L}{\overline{v}} \simeq L \left(1 + \frac{\overline{m^2}}{2E^2}\right) \qquad \text{and} \qquad \Delta t \sim \sigma_x\,, \tag{7.46}$$

where $\overline{v} = 1 - \overline{m^2}/2E^2$ is the average group velocity, $\overline{m^2}$ is the average of the squared neutrino masses, and σ_x is given by the spatial uncertainties of the production and detection processes summed in quadrature [528] (the spatial uncertainty of the production process determines the size of the massive neutrino wave packets). The correction $L\overline{m^2}/2E^2$ to $t = L$ in eqn (7.46) can be neglected, because it gives corrections to the oscillation phases which are of higher order in the very small ratios m_k^2/E^2. The corrections due to $\Delta t \sim \sigma_x$ are also negligible, because in all real experiments σ_x is much smaller than the oscillation length $L_{kj}^{\rm osc} = 4\pi E/\Delta m_{kj}^2$; otherwise oscillations cannot be observed [660, 533, 225, 526]. One can summarize these arguments by saying that the approximation $t = L$ is correct because the phase of the oscillations is practically constant over the interval of time in which the massive neutrino wave packets overlap in the detection process.

7.2 Antineutrino case

As we have discussed in the introduction to this chapter, flavor neutrinos are produced in weak interaction processes through the action of the leptonic charged-current in eqn (7.2), which contains the creation operators of massive neutrinos. Antineutrinos $\bar{\nu}_\alpha$ with flavor $\alpha = e, \mu, \tau$ are similarly produced in charged-current (CC) weak interaction processes from a charged antilepton ℓ_α^+ (i.e. $\ell_\alpha^+ \to \bar{\nu}_\alpha$ transitions) or together with a charged lepton ℓ_α^- (i.e. creation of a $\ell_\alpha^-\ \bar{\nu}_\alpha$ pair), through the action of the Hermitian conjugate of the leptonic charged-current in eqn (7.2),

$$j_{W,{\rm L}}^{\rho\,\dagger} = 2 \sum_{\alpha=e,\mu,\tau} \overline{\ell_{\alpha L}}\, \gamma^\rho\, \nu_{\alpha L} = 2 \sum_{\alpha=e,\mu,\tau} \sum_k U_{\alpha k}\, \overline{\ell_{\alpha L}}\, \gamma^\rho\, \nu_{k L}\,, \tag{7.47}$$

which is included in the charged-current leptonic interaction Lagrangian in eqn (7.1). In fact, the Hermitian-conjugated leptonic charged-current in eqn (7.47)

contains, through the adjoint charged lepton field $\overline{\ell_\alpha}$, destruction operators of ℓ_α^+ for the generation of $\ell_\alpha^+ \to \bar{\nu}_\alpha$ transitions, and creation operators of ℓ_α^- for the creation of $\ell_\alpha^- \; \bar{\nu}_\alpha$ pairs.

In the case of Dirac neutrinos, the Fourier expansion of the field operator ν_{kL} (see eqn (2.139)),

$$\nu_{kL}(x) = \int \frac{\mathrm{d}^3 p}{(2\pi)^3 \, 2E} \sum_{h=\pm 1} \left[a^{(h)}_{\nu_k}(p) \, u^{(h)}_{\nu_k L}(p) \, e^{-ip \cdot x} + b^{(h)\dagger}_{\nu_k}(p) \, v^{(h)}_{\nu_k L}(p) \, e^{ip \cdot x} \right] , \tag{7.48}$$

contains creation operators $b^{(h)}_{\nu_k}(p)$ of antineutrinos with mass m_k. In neutrino oscillation experiments, the energies and momenta of the particles involved in the neutrino production process are not measured with a degree of accuracy which would allow one to determine, through energy–momentum conservation, which massive neutrino is emitted. In this case, the Hermitian-conjugated leptonic charged-current in eqn (7.47) produces flavor antineutrinos $\bar{\nu}_\alpha$ which are superpositions of massive antineutrinos $\bar{\nu}_k$ with weights proportional to $U_{\alpha k}$. Neglecting additional coefficients due to the effect of the difference of the neutrino masses in the interaction process (see subsection 8.1.1), these flavor antineutrinos are described by the standard flavor antineutrino states

$$|\bar{\nu}_\alpha\rangle = \sum_k U_{\alpha k} \, |\bar{\nu}_k\rangle \qquad (\alpha = e, \mu, \tau) \, . \tag{7.49}$$

It is to be noted that the coefficients of the massive neutrino components of flavor antineutrinos are simply related to the corresponding coefficients of the massive neutrino components of flavor antineutrinos by complex conjugation.

In the case of Majorana neutrinos, there is no difference between neutrinos and antineutrinos. However, as we have explained in section 6.2.3, it is customary, by convention, to call Majorana neutrinos with negative helicity *neutrinos* and Majorana neutrinos with positive helicity *antineutrinos*. Hence, the standard flavor neutrino states in eqn (7.4) describe Dirac or Majorana neutrinos with negative helicity and the states in eqn (7.49) describe Dirac antineutrinos with positive helicity or Majorana neutrinos with positive helicity.

Let us now consider the probability of $\bar{\nu}_\alpha \to \bar{\nu}_\beta$ oscillations. Since the kinematical properties of massive antineutrinos are identical to those of neutrinos, the derivation of the probability of $\bar{\nu}_\alpha \to \bar{\nu}_\beta$ oscillations follows the same lines as that of $\nu_\alpha \to \nu_\beta$ oscillations presented in the previous section 7.1, the only difference being that in this case we start with the flavor antineutrino states in eqn (7.49) in which the elements of the mixing matrix are complex conjugated with respect to the flavor neutrino states in eqn (7.4). Applying the same transformation to the neutrino oscillation probability in eqn (7.23), we obtain the antineutrino oscillation probability

$$P_{\bar{\nu}_\alpha \to \bar{\nu}_\beta}(L, E) = \sum_{k,j} U_{\alpha k} \, U^*_{\beta k} \, U^*_{\alpha j} \, U_{\beta j} \, \exp\left(-i \, \frac{\Delta m^2_{kj} L}{2E} \right) . \tag{7.50}$$

In particular, we note that the oscillation length of antineutrinos is the same as that of neutrinos, given in eqn (7.31), since it depends only on the same kinematical properties of massive neutrinos and antineutrinos. Writing the antineutrino oscillation probability as

$$P_{\bar{\nu}_\alpha \to \bar{\nu}_\beta}(L,E) = \delta_{\alpha\beta} - 4 \sum_{k>j} \Re\mathfrak{e}\left[U^*_{\alpha k}\, U_{\beta k}\, U_{\alpha j}\, U^*_{\beta j}\right] \, \sin^2\left(\frac{\Delta m^2_{kj} L}{4E}\right) - 2 \sum_{k>j} \Im\mathfrak{m}\left[U^*_{\alpha k}\, U_{\beta k}\, U_{\alpha j}\, U^*_{\beta j}\right] \, \sin\left(\frac{\Delta m^2_{kj} L}{2E}\right) , \tag{7.51}$$

one can see that it differs from the corresponding neutrino oscillation probability in eqn (7.38) only in the sign of the terms depending on the imaginary parts of the quartic products of the elements of the mixing matrix.

7.3 CPT, CP, and T transformations

Physical neutrinos and antineutrinos are related by a CP transformation which interchanges neutrinos with antineutrinos and reverses the helicity[36] (see subsection 2.11.3):

$$\nu_\alpha \overset{\text{CP}}{\longleftrightarrow} \bar{\nu}_\alpha \, . \tag{7.52}$$

Moreover, a T transformation interchanges the initial and final states. Therefore, as schematized in Fig. 7.1, a CP transformation interchanges the $\nu_\alpha \to \nu_\beta$ and $\bar{\nu}_\alpha \to \bar{\nu}_\beta$ channels,

$$\nu_\alpha \to \nu_\beta \overset{\text{CP}}{\longleftrightarrow} \bar{\nu}_\alpha \to \bar{\nu}_\beta \, . \tag{7.53}$$

A T transformation interchanges the $\nu_\alpha \to \nu_\beta$ and $\nu_\beta \to \nu_\alpha$ channels,

$$\nu_\alpha \to \nu_\beta \overset{\text{T}}{\longleftrightarrow} \nu_\beta \to \nu_\alpha \, , \tag{7.54}$$

or the $\bar{\nu}_\alpha \to \bar{\nu}_\beta$ and $\bar{\nu}_\beta \to \bar{\nu}_\alpha$ channels,

$$\bar{\nu}_\alpha \to \bar{\nu}_\beta \overset{\text{T}}{\longleftrightarrow} \bar{\nu}_\beta \to \bar{\nu}_\alpha \, . \tag{7.55}$$

Finally, CPT interchanges the $\nu_\alpha \to \nu_\beta$ and $\bar{\nu}_\beta \to \bar{\nu}_\alpha$ channels,

$$\nu_\alpha \to \nu_\beta \overset{\text{CPT}}{\longleftrightarrow} \bar{\nu}_\beta \to \bar{\nu}_\alpha \, . \tag{7.56}$$

[36] As discussed in the previous section 7.2, in the case of Majorana neutrinos, where the C transformation coincides with the identity, it is conventional to call *neutrinos* the states with negative helicity and *antineutrinos* the states with positive helicity.

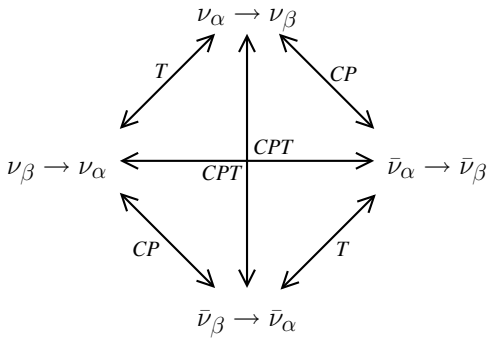

FIG. 7.1. Scheme of the CPT, CP, and T transformations that relate different flavor transition channels.

7.3.1 CPT

The CPT transformation is a symmetry of any local quantum field theory (see Refs. [988]), such as the SM, presented in chapter 3, and its extensions with the inclusion of neutrino masses, discussed in chapter 6. Since the theory of neutrino oscillations which we consider in this book is formulated in the framework of a local quantum field theory, CPT is a symmetry of the oscillation probabilities. Hence, we have

$$P_{\nu_\alpha \to \nu_\beta} = P_{\bar{\nu}_\beta \to \bar{\nu}_\alpha} \,. \tag{7.57}$$

In fact, we have, from eqn (7.50),

$$P_{\bar{\nu}_\beta \to \bar{\nu}_\alpha}(L,E) = \sum_{k,j} U_{\beta k}\, U^*_{\alpha k}\, U^*_{\beta j}\, U_{\alpha j}\, \exp\left(-i\,\frac{\Delta m^2_{kj} L}{2E}\right) , \tag{7.58}$$

which coincides with $P_{\nu_\alpha \to \nu_\beta}(L,E)$ in eqn (7.23). The equality in eqn (7.57) is also easily verified by noting that the probability in eqn (7.58) is invariant under a CP transformation ($\bar{\nu}_\beta \to \bar{\nu}_\alpha \Rightarrow \nu_\beta \to \nu_\alpha$) which changes $U \leftrightarrows U^*$, followed by a T transformation ($\nu_\beta \to \nu_\alpha \Rightarrow \nu_\alpha \to \nu_\beta$) which changes $\alpha \leftrightarrows \beta$.

A special case of the equality in eqn (7.57) is the equality of the survival probabilities of neutrinos and antineutrinos,

$$P_{\nu_\alpha \to \nu_\alpha} = P_{\bar{\nu}_\alpha \to \bar{\nu}_\alpha} \,, \tag{7.59}$$

which has important phenomenological implications.

It is possible, however, that the description of nature through local Quantum Field Theories is approximate. In this case, there may be small violations of the CPT symmetry. Neutrino oscillations experiments could reveal such violations by measuring a nonzero value of the CPT asymmetry

$$A^{\rm CPT}_{\alpha\beta} = P_{\nu_\alpha \to \nu_\beta} - P_{\bar{\nu}_\beta \to \bar{\nu}_\alpha} \,. \tag{7.60}$$

7.3.2 CP

As shown in eqns (7.52), (7.53) and Fig. 7.1, the CP transformation interchanges neutrinos with negative helicity and antineutrinos with positive helicity, transforming the $\nu_\alpha \to \nu_\beta$ channel into the $\bar{\nu}_\alpha \to \bar{\nu}_\beta$ channel. As we have discussed in section 6.1.2, in the case of three-neutrino mixing, the mixing matrix is, in general, complex and leads to violations of the CP symmetry. Such violations can be revealed in neutrino oscillation experiments by measuring the CP asymmetry

$$A^{\rm CP}_{\alpha\beta} = P_{\nu_\alpha\to\nu_\beta} - P_{\bar{\nu}_\alpha\to\bar{\nu}_\beta} \,. \tag{7.61}$$

The CPT symmetry implies that the CP asymmetry is antisymmetric in the flavor indices α and β,

$$A^{\rm CP}_{\alpha\beta} = -A^{\rm CP}_{\beta\alpha} \,, \tag{7.62}$$

because the CPT relation in eqn (7.57), $P_{\nu_\alpha\to\nu_\beta} = P_{\bar{\nu}_\beta\to\bar{\nu}_\alpha}$, also implies $P_{\bar{\nu}_\alpha\to\bar{\nu}_\beta} = P_{\nu_\beta\to\nu_\alpha}$. Hence, it is clear that a CP asymmetry can be measured only in transitions between different flavors.

As discussed in section 7.2, the oscillation probabilities of neutrinos and antineutrinos are related by complex conjugation of the elements of the mixing matrix. Confronting eqns (7.38) and (7.51), one can see that they differ only in the sign of the terms depending on the imaginary parts of the quartic products of the elements of the mixing matrix. Thus, only these terms contribute to the CP asymmetry, leading to

$$A^{\rm CP}_{\alpha\beta}(L,E) = 4\sum_{k>j} \Im\mathfrak{m}\left[U^*_{\alpha k}\, U_{\beta k}\, U_{\alpha j}\, U^*_{\beta j}\right] \sin\left(\frac{\Delta m^2_{kj} L}{2E}\right) \,. \tag{7.63}$$

This expression confirms that a CP asymmetry can be measured only in the transitions between different flavors, since, for $\alpha = \beta$, the imaginary parts in eqn (7.63) vanish.

Since the quartic products of elements of the mixing matrix in eqn (7.63) depend only on the Dirac phases in the mixing matrix, as we have discussed in section 6.2.1, CP violation in neutrino oscillations depend only on the Dirac phases in the mixing matrix.

A characteristic of the CP asymmetry in eqn (7.63), which is important for practical applications, is that its average over the distance L or the energy E vanishes. Therefore, in order to be able to measure CP violations in neutrino oscillations, experiments must be sensitive to the oscillatory behavior of the neutrino and antineutrino transition probabilities. This means that the distance L and energy E must be such that at least one of the phases $\Delta m^2_{kj} L/2E$ is of order one. If all the phases are much smaller than unity, the transition probabilities are too small to be measurable, whereas if all the phases are much larger than unity, the average of the CP asymmetry in eqn (7.63) over the uncertainty in L and E washes out all the sine functions. However, as we will see in section 7.7, the phase of order one should not be generated by the largest squared-mass difference, because in that case the effective CP asymmetries are identically zero.

7.3.3 T

If CPT is a symmetry of nature, the violation of CP symmetry implies the violation of T symmetry, which interchanges the initial and final states in neutrino oscillations (see eqns (7.54) and (7.55) and Fig. 7.1), as in other processes. In neutrino oscillation experiments it is possible to observe T violations by measuring the T asymmetries of neutrinos and antineutrinos

$$A^{\mathrm{T}}_{\alpha\beta} = P_{\nu_\alpha \to \nu_\beta} - P_{\nu_\beta \to \nu_\alpha} \,, \tag{7.64}$$

$$\bar{A}^{\mathrm{T}}_{\alpha\beta} = P_{\bar{\nu}_\alpha \to \bar{\nu}_\beta} - P_{\bar{\nu}_\beta \to \bar{\nu}_\alpha} \,. \tag{7.65}$$

The CPT relation in eqn (7.57) implies that

$$A^{\mathrm{T}}_{\alpha\beta} = -\bar{A}^{\mathrm{T}}_{\alpha\beta} = A^{\mathrm{CP}}_{\alpha\beta} \,. \tag{7.66}$$

In this case, measuring a CP asymmetry is equivalent to measuring a T asymmetry. As noted for the case of CP violation, T violations in neutrino oscillations depend only on the Dirac phases of the mixing matrix. In order to measure T violations, one should carry out neutrino oscillation experiments which are sensitive to the oscillatory behavior of the flavor transition probabilities.

7.4 Two-neutrino mixing

Two-neutrino mixing is an approximation in which only two massive neutrinos out of three are considered. That is, one neglects the coupling of the flavor neutrinos with the third massive neutrino that exists in nature. This approximation is very useful in practice for two reasons:

1. The oscillation formulas in the case of two-neutrino mixing are much simpler and depend on fewer parameters than in the case of three-neutrino mixing.
2. Since many experiments are not sensitive to the influence of three-neutrino mixing, the data can be analyzed by using an effective model with two-neutrino mixing.

In the case of two-neutrino mixing, we consider two flavor neutrinos ν_α and ν_β, which can be pure flavor neutrinos ($\alpha, \beta = e, \mu$ or $\alpha, \beta = e, \tau$ or $\alpha, \beta = \mu, \tau$) or linear combinations of pure flavor neutrinos (for example, $\nu_\alpha = \nu_e$ and $\nu_\beta = c_\mu \nu_\mu + c_\tau \nu_\tau$, with $c^2_\mu + c^2_\tau = 1$ in electron neutrino disappearance experiments or $\nu_e \to \nu_{\mu,\tau}$ experiments where ν_μ and ν_τ are not distinguished). The two flavor neutrino states are linear superpositions of the two massive neutrinos ν_1 and ν_2 with coefficients given by the elements of the two-neutrino effective mixing matrix

$$U = \begin{pmatrix} \cos\vartheta & \sin\vartheta \\ -\sin\vartheta & \cos\vartheta \end{pmatrix} \,, \tag{7.67}$$

where ϑ is the mixing angle, with a value in the interval $0 \leq \vartheta \leq \pi/2$. In the case of two-neutrino mixing, there is only one squared-mass difference:

$$\Delta m^2 \equiv \Delta m^2_{21} \equiv m^2_2 - m^2_1 \,. \tag{7.68}$$

For convenience, we define ν_1 as the lightest of the two massive neutrinos, so that Δm^2 is positive[37].

From eqn (7.23), it is straightforward to derive the expression for the probability of $\nu_\alpha \to \nu_\beta$ transitions with $\alpha \neq \beta$:

$$P_{\nu_\alpha \to \nu_\beta}(L,E) = \frac{1}{2}\,\sin^2 2\vartheta \left[1 - \cos\left(\frac{\Delta m^2 L}{2E}\right)\right] \qquad (\alpha \neq \beta)\,, \tag{7.69}$$

or, equivalently,

$$P_{\nu_\alpha \to \nu_\beta}(L,E) = \sin^2 2\vartheta\, \sin^2\left(\frac{\Delta m^2 L}{4E}\right) \qquad (\alpha \neq \beta)\,. \tag{7.70}$$

In the case $\alpha = \beta$, the *survival probability* $P_{\nu_\alpha \to \nu_\alpha}(L,E)$ is easily obtained by unitarity from the transition probability in eqn (7.70):

$$P_{\nu_\alpha \to \nu_\alpha}(L,E) = 1 - P_{\nu_\alpha \to \nu_\beta}(L,E) = 1 - \sin^2 2\vartheta\, \sin^2\left(\frac{\Delta m^2 L}{4E}\right)\,. \tag{7.71}$$

From eqn (7.31), the oscillation length in this case is given by

$$L^{\rm osc} = \frac{4\pi E}{\Delta m^2}\,, \tag{7.72}$$

and the average transition probability in eqn (7.33), which is the same as the incoherent transition probability in eqn (7.32), becomes

$$\langle P_{\nu_\alpha \to \nu_\beta} \rangle = \frac{1}{2}\,\sin^2 2\vartheta \qquad (\alpha \neq \beta)\,. \tag{7.73}$$

This expression can simply be derived from eqn (7.69) by noting that the average of the cosine function is zero.

One can see from eqn (7.70) that the mixing angle dependence of the transition probability is expressed by $\sin^2 2\vartheta$, which is symmetric under the exchange $\vartheta \leftrightarrows \pi/2 - \vartheta$. Since the allowed range of ϑ is $0 \leq \vartheta \leq \pi/2$, there is a degeneracy of the transition probability for ϑ and $\pi/2 - \vartheta$. However, it is important to keep in mind that the two possibilities correspond to two physically different mixings: if

[37] Some authors prefer to constrain the mixing angle in the interval $0 \leq \vartheta \leq \pi/4$, considering positive and negative Δm^2. The usefulness of this convention stems from the consideration that $0 \leq \vartheta \leq \pi/4$ corresponds to $0 \leq \sin^2 2\vartheta \leq 1$. Since the flavor transition probability in eqn (7.69) depends on the mixing angle through $\sin^2 2\vartheta$, considering $0 \leq \vartheta \leq \pi/4$ covers all the possibilities, leaving a complete uncertainty on the sign of Δm^2. We did not adopt such a convention because it may give the false impression that there is a discontinuity for $\vartheta = \pi/4$, related to the change of sign of Δm^2. This inconvenience becomes evident [359] in the case of neutrino oscillations in matter (see section 9.3), where the mixing-angle dependence of the flavor transition probability is not limited to $\sin^2 2\vartheta$. Hence, our convention is more appropriate for a clear unified treatment of neutrino oscillations in vacuum and in matter. In fact, it is adopted by most authors in the latest analyses of solar neutrino data, in which the mixing is quantified through $\tan^2\vartheta$ (see section 10.10).

$\vartheta < \pi/4$ the electron neutrino is composed more of ν_1 than ν_2 and vice versa for ν_μ; if $\vartheta > \pi/4$ the electron neutrino is composed more of ν_2 than ν_1 and vice versa for ν_μ. The degeneracy is resolved in neutrino oscillations in matter, as will be explained in section 9.3.

For the analyses of the data of reactor oscillation experiments, in which $E \sim 1\,\text{MeV}$, as well as those of accelerator oscillation experiments, in which $E \sim 1\,\text{GeV}$, it is convenient to write the transition probability in eqn (7.70) as

$$\begin{aligned} P_{\nu_\alpha \to \nu_\beta}(L,E) &= \sin^2 2\vartheta \, \sin^2\left(1.27\,\frac{\Delta m^2[\text{eV}^2]\,L[\text{m}]}{E[\text{MeV}]}\right) \\ &= \sin^2 2\vartheta \, \sin^2\left(1.27\,\frac{\Delta m^2[\text{eV}^2]\,L[\text{km}]}{E[\text{GeV}]}\right) . \end{aligned} \tag{7.74}$$

and the oscillation length as

$$L^{\text{osc}} = 2.47\,\frac{E\,[\text{MeV}]}{\Delta m^2\,[\text{eV}^2]}\,\text{m} = 2.47\,\frac{E\,[\text{GeV}]}{\Delta m^2\,[\text{eV}^2]}\,\text{km}\,. \tag{7.75}$$

The behavior of the transition probability in eqn (7.70) for $\sin^2 2\vartheta = 1$ as a function of $L/E\,[\text{km/GeV}]\,\Delta m^2\,[\text{eV}^2]$ is shown by the dashed line in Fig. 7.2. For fixed values of the squared-mass difference Δm^2 and of the energy E, the axis represents the distance L. The oscillation length in eqn (7.75) corresponds to the location of the first dip of the transition probability at $L/E\,[\text{km/GeV}]\,\Delta m^2\,[\text{eV}^2] = 2.47$, where the phase in the cosine function in eqn (7.69) is equal to 2π and the phase in the sine function in eqn (7.70) is equal to π. The transition probability is very small for $L \ll L^{\text{osc}}$ and oscillates very rapidly for $L \gg L^{\text{osc}}$ in the logarithmic scale of L.

From the absence of any phase in the two-neutrino effective mixing matrix in eqn (7.67), it is clear that there are no CP or T violations and the transition probabilities of neutrinos and antineutrinos as well as the probabilities of direct and inverted channels are all equal:

$$P_{\nu_\alpha \to \nu_\beta}(L,E) = P_{\nu_\beta \to \nu_\alpha}(L,E) = P_{\bar\nu_\alpha \to \bar\nu_\beta}(L,E) = P_{\bar\nu_\beta \to \bar\nu_\alpha}(L,E)\,. \tag{7.76}$$

7.5 Types of neutrino oscillation experiments

The discussion in the previous section helps us to understand the usual classification of the different types of neutrino oscillation experiments.

Neutrino oscillation experiments are divided into:

Appearance experiments. These experiments measure transitions between different neutrino flavors. If the final flavor to be searched for in the detector is not present in the initial beam, the background can be very small. In this case, an experiment can be sensitive to rather small values of the mixing angle.

Disappearance experiments. These experiments measure the survival probability of a neutrino flavor by counting the number of interactions in the detector

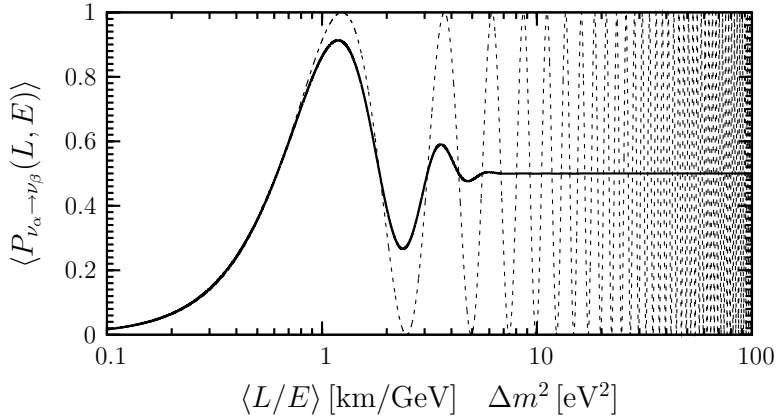

FIG. 7.2. Probability of $\nu_\alpha \to \nu_\beta$ transitions for $\sin^2 2\vartheta = 1$ as a function of $\langle L/E \rangle$ [km/GeV] Δm^2 [eV^2]. The average ratio $\langle L/E \rangle$ can also be expressed in units [m/MeV]. Solid line: transition probability averaged over a Gaussian L/E distribution with $\sigma_{L/E} = 0.2 \langle L/E \rangle$ (see eqn (7.93)). Dashed line: unaveraged transition probability (see eqn (7.70)), with $L/E = \langle L/E \rangle$.

and comparing it with the expected one. Since, even in the absence of oscillations, the number of detected events has statistical fluctuations, it is very difficult to reveal a small disappearance. Therefore, in this type of experiment, it is hard to measure small values of the mixing angle.

In the simplest case of two-neutrino mixing, an important characteristic of neutrino oscillations is that the transitions to different flavors cannot be measured if

$$\frac{\Delta m^2 L}{2E} \ll 1 \,. \tag{7.77}$$

On the other hand, for

$$\frac{\Delta m^2 L}{2E} \gg 1 \tag{7.78}$$

only the average transition probability in eqn (7.73) is observable, yielding information only on $\sin^2 2\vartheta$.

Since the value of Δm^2 is fixed by nature, different experiments can be designed in order to be sensitive to different values of Δm^2, by choosing appropriate values of the ratio L/E. The so-called *sensitivity* to Δm^2 of an experiment is the value of Δm^2 for which

$$\frac{\Delta m^2 L}{2E} \sim 1 \,. \tag{7.79}$$

Different types of neutrino oscillation experiments are traditionally classified depending on the average value of the ratio L/E for an experiment, which determines its sensitivity to Δm^2 through eqn (7.79) (see Table 7.1):

Short BaseLine experiments (SBL). They are divided as follows:

TABLE 7.1. Types of neutrino oscillation experiments with their typical source–detector distance, energy, and sensitivity to Δm^2, which is given by $E[\text{MeV}]/L[\text{m}] = E[\text{GeV}]/L[\text{km}]$ (see eqn (7.79)).

Type of experiment	L	E	Δm^2 sensitivity
Reactor SBL	$\sim 10\,\text{m}$	$\sim 1\,\text{MeV}$	$\sim 0.1\,\text{eV}^2$
Accelerator SBL (Pion DIF)	$\sim 1\,\text{km}$	$\gtrsim 1\,\text{GeV}$	$\gtrsim 1\,\text{eV}^2$
Accelerator SBL (Muon DAR)	$\sim 10\,\text{m}$	$\sim 10\,\text{MeV}$	$\sim 1\,\text{eV}^2$
Accelerator SBL (Beam Dump)	$\sim 1\,\text{km}$	$\sim 10^2\,\text{GeV}$	$\sim 10^2\,\text{eV}^2$
Reactor LBL	$\sim 1\,\text{km}$	$\sim 1\,\text{MeV}$	$\sim 10^{-3}\,\text{eV}^2$
Accelerator LBL	$\sim 10^3\,\text{km}$	$\gtrsim 1\,\text{GeV}$	$\gtrsim 10^{-3}\,\text{eV}^2$
ATM	20–$10^4\,\text{km}$	0.5–$10^2\,\text{GeV}$	$\sim 10^{-4}\,\text{eV}^2$
Reactor VLB	$\sim 10^2\,\text{km}$	$\sim 1\,\text{MeV}$	$\sim 10^{-5}\,\text{eV}^2$
Accelerator VLB	$\sim 10^4\,\text{km}$	$\gtrsim 1\,\text{GeV}$	$\gtrsim 10^{-4}\,\text{eV}^2$
SOL	$\sim 10^{11}\,\text{km}$	0.2–$15\,\text{MeV}$	$\sim 10^{-12}\,\text{eV}^2$

Reactor SBL. These are experiments that utilize large isotropic fluxes of electron antineutrinos produced in nuclear reactors by β^--decays of heavy nuclei (mainly fission fragments of ^{235}U, ^{238}U, ^{239}Pu, ^{241}Pu). A typical energy of reactor ν_e's is of the order of a few MeV and the source–detector distance in the reactor SBL experiments is several tens of meters. The range of L/E covered by the reactor SBL experiments and their sensitivity to Δm^2 are

$$\frac{L}{E} \lesssim 10\,\text{m/MeV} \quad \Longrightarrow \quad \Delta m^2 \gtrsim 0.1\,\text{eV}^2\,. \tag{7.80}$$

Since the antineutrino energy is too low to produce μ's or τ's, only the survival probability of $\bar{\nu}_e$'s can be measured by detecting, in a liquid scintillator, the inverse β-decay reaction

$$\bar{\nu}_e + p \to n + e^+\,, \tag{7.81}$$

with a threshold $E_{\text{th}} = 1.8\,\text{MeV}$. Experiments of this type which have been performed in the past are: ILL [710], Gosgen [1082], Rovno [32], Krasnoyarsk [1037], Bugey [363], Savannah River [563].

Accelerator SBL. These are experiments with beams of neutrinos produced by decay of pions, kaons, and muons created by a proton beam hitting a target. They can be divided as:

Pion Decay In Flight (DIF). These are the experiments with a neutrino beam composed mainly of muon neutrinos produced by the decay of pions and kaons initially produced by a proton beam hitting a target. The pions and kaons are allowed to decay in a decay tunnel of length of the order of 100 m. The beam is composed of ν_μ's or $\bar{\nu}_\mu$'s, depending on the polarity of the horn which focalizes the pions and kaons. In the case of a ν_μ beam

produced by $\pi^+, K^+ \to \mu^+ + \nu_\mu$, there are about 1% of $\bar{\nu}_\mu$'s and about 1% of ν_e's, which are mainly due to $\mu^+ \to e^+ + \nu_e + \bar{\nu}_\mu$ decays[38]. The typical energy of the neutrinos is of the order of a few GeV, but can be much larger, depending on the energy of the proton beam. The typical source–detector distance in the accelerator SBL experiments is of the order of 1 km. The range of L/E covered by these experiments and their sensitivity to Δm^2 are

$$\frac{L}{E} \lesssim 1\,\text{km/GeV} \quad \Longrightarrow \quad \Delta m^2 \gtrsim 1\,\text{eV}^2\,. \tag{7.82}$$

In the case of $\nu_\mu \to \nu_\tau$ and $\bar{\nu}_\mu \to \bar{\nu}_\tau$ transitions, the energy must be about one order of magnitude larger in order to have sufficient τ productions (the τ production threshold is about 3.5 GeV; see Table 5.2), leading to $L/E \lesssim 0.1\,\text{km/GeV}$ and a sensitivity to $\Delta m^2 \gtrsim 10\,\text{eV}^2$. Experiments of this type which have been performed in the past are: BEBC [89] ($\nu_\mu \to \nu_e$), FNAL-E531 [1030] ($\nu_\mu \to \nu_\tau$), CDHSW [396] ($\overset{(-)}{\nu}_\mu \to \overset{(-)}{\nu}_\mu$), CCFR ($\overset{(-)}{\nu}_\mu \to \overset{(-)}{\nu}_\mu$ [983], $\overset{(-)}{\nu}_\mu \to \overset{(-)}{\nu}_\tau$ [789], $\overset{(-)}{\nu}_\mu \to \overset{(-)}{\nu}_e$ [910], $\overset{(-)}{\nu}_e \to \overset{(-)}{\nu}_\tau$ [823]), CHARM [212] ($\nu_\mu \to \nu_\mu$, $\nu_\mu \to \nu_e$, $\nu_\mu \to \nu_\tau$), BNL-E776 [265] ($\overset{(-)}{\nu}_\mu \to \overset{(-)}{\nu}_e$), CHORUS [422] ($\nu_\mu \to \nu_\tau$, $\nu_e \to \nu_\tau$), NOMAD [116] ($\nu_\mu \to \nu_\tau$, $\nu_e \to \nu_\tau$, $\nu_\mu \to \nu_e$), LSND [121] ($\nu_\mu \to \nu_e$), NuTeV [130] ($\overset{(-)}{\nu}_\mu \to \overset{(-)}{\nu}_e$).

Muon Decay At Rest (DAR). These are lower energy experiments with a beam composed of muon antineutrinos coming from the decay

$$\mu^+ \to e^+ + \nu_e + \bar{\nu}_\mu \tag{7.83}$$

of the μ^+ produced in the pion decay

$$\pi^+ \to \mu^+ + \nu_\mu \tag{7.84}$$

(the π^- are mostly absorbed by nuclei) and stopped in the target. These $\bar{\nu}_\mu$'s have energy of the order of several tens of MeV and can be used for measuring $\bar{\nu}_\mu \to \bar{\nu}_e$ transitions, because $\bar{\nu}_e$ are not present in the final products of π^+ and μ^+-decay. These experiments have a typical source–detector distance of the order of several tens of meters, with a range of L/E and a sensitivity to Δm^2 given by

$$\frac{L}{E} \lesssim 1\,\text{m/MeV} \quad \Longrightarrow \quad \Delta m^2 \gtrsim 1\,\text{eV}^2\,. \tag{7.85}$$

Experiments of this type that have been performed in the past are the $\bar{\nu}_\mu \to \bar{\nu}_e$ experiments LAMPF-0645 [460], LSND [37], KARMEN [105].

[38] Since pions and muons are ultrarelativistic and have about the same time for decaying in the decay tunnel, the ratio of the numbers of muon and pion decays is approximately equal to the ratio of the pion and muon lifetimes, which is about 1% (see eqns (A.155) and (A.162)). The small branching ratio of the $\pi^+ \to e^+ + \nu_e$ decay channel increases the electron neutrino fraction only by about 0.01% (see eqn (5.60)). Kaons, which are typically about 10% of pions, have a branching ratio of about 5% for $K^+ \to \pi^0 + e^+ + \nu_e$ decays, which give an additional contribution of about 0.5% to the ν_e contamination.

Beam Dump. Also called *prompt* neutrino experiments. In these experiments a proton beam with very high energy, of the order of some hundreds of GeV, is completely stopped in a thick target, called the *beam dump*, where the proton nucleon interactions generate heavy hadrons. The charmed heavy hadrons decay promptly with practically equal branching ratios into electrons and muons, emitting equal fluxes of electron and muon neutrinos with energies of the order of 10^2 GeV. A detector at a distance of the order of 1 km can measure the ratio of the electron and muon neutrino fluxes, whose deviations from unity would signal the presence of oscillations. The typical range of L/E and sensitivity to Δm^2 are given by

$$\frac{L}{E} \lesssim 10^{-2}\,\mathrm{m/MeV} \quad \Longrightarrow \quad \Delta m^2 \gtrsim 10^2\,\mathrm{eV}^2\,. \tag{7.86}$$

Experiments of this type that have been performed in the past are: BEBC [465, 559], CHARM [388], CDHSW [208].

Long BaseLine experiments (LBL). These are experiments which have sources similar to SBL experiments, but the source–detector distance is about two or three orders of magnitude larger. LBL experiments are classified as follows:

Reactor LBL. These are reactor neutrino experiments in which the source–detector distance is of the order of 1 km. The range of L/E covered by these experiments and their sensitivity to Δm^2 are

$$\frac{L}{E} \lesssim 10^{3}\,\mathrm{m/MeV} \quad \Longrightarrow \quad \Delta m^2 \gtrsim 10^{-3}\,\mathrm{eV}^2\,. \tag{7.87}$$

Experiments of this type which have been performed in the past are: CHOOZ [100] and Palo Verde [255]. Several future experiments are under study or in preparation: Double CHOOZ [104], KASKA [994], and others (see the reviews in Refs. [87, 557]).

Accelerator LBL. These are neutrino experiments with a muon neutrino or antineutrino beam produced by the decay in flight of pions and kaons created by shooting a proton beam to a target. The source–detector distance is about 10^2–10^3 km, leading to a range of L/E and a sensitivity to Δm^2 given by

$$\frac{L}{E} \lesssim 10^{3}\,\mathrm{km/GeV} \quad \Longrightarrow \quad \Delta m^2 \gtrsim 10^{-3}\,\mathrm{eV}^2\,. \tag{7.88}$$

The only experiment of this type which has produced results is K2K, which is still running. The results obtained so far have been published in Ref. [48, 46, 66] for the $\nu_\mu \to \nu_\mu$ channel and in Ref. [47] for the $\nu_\mu \to \nu_e$ channel. The MINOS experiment [131] ($\nu_\mu \to \nu_\mu$, $\nu_\mu \to \nu_e$) started in 2005. Two future experiments are under preparation: ICARUS [101] ($\nu_\mu \to \nu_\tau$, $\nu_\mu \to \nu_e$), OPERA [577] ($\nu_\mu \to \nu_\tau$). Another experiment called T2K [633] ($\nu_\mu \to \nu_\mu$, $\nu_\mu \to \nu_e$) with a neutrino superbeam, i.e. a conventional accelerator neutrino beam with much larger intensity, is being planned at Tokai, in Japan.

ATMospheric neutrino experiments (ATM). Primary cosmic rays interact with the upper layers of the atmosphere producing a large flux of pions and kaons which decay in the atmosphere into muons and neutrinos. Many muons further decay into electrons and neutrinos before hitting the ground. Atmospheric neutrino experiments detect these neutrinos. The energy of detectable atmospheric neutrinos cover a very wide range, from about 500 MeV to about 100 GeV. The source–detector distance ranges from about 20 km for neutrinos coming from above, to about 1.3×10^4 km for neutrinos coming from below, initially produced on the other side of the Earth. Therefore, in atmospheric neutrino experiments, typical values of L/E and the associated sensitivity to Δm^2 are

$$\frac{L}{E} \lesssim 10^4 \,\mathrm{km/GeV} \quad \Longrightarrow \quad \Delta m^2 \gtrsim 10^{-4} \,\mathrm{eV}^2 \,. \tag{7.89}$$

Atmospheric neutrino experiments which have been performed in the past are: Kamiokande [474], IMB [199], NUSEX [34], Frejus [352], Super-Kamiokande [110], MACRO [84], Soudan-2 [922]. The Super-Kamiokande and Soudan-2 experiments are still operating. Also the MINOS detector, which started in 2005, is sensitive to atmospheric neutrinos [745].

Very Long-Baseline experiments (VLB). These are experiments with a source–detector distance larger than LBL experiments by one or two orders of magnitude. They are:

Reactor VLB. These experiments measure the combined neutrino flux of many reactors at a distance of the order of 100 km, with a range of L/E and a sensitivity to Δm^2 given by

$$\frac{L}{E} \lesssim 10^5 \,\mathrm{m/MeV} \quad \Longrightarrow \quad \Delta m^2 \gtrsim 10^{-5} \,\mathrm{eV}^2 \,. \tag{7.90}$$

Only one experiment, KamLAND [398], is still in operation. In the future, the Borexino [1008] experiment may be able to perform as a reactor VLB experiment.

Accelerator VLB. These are accelerator neutrino experiments with a source–detector distance of the order of several thousands of km, comparable with the diameter of the Earth. They cover the range of L/E and the sensitivity to Δm^2 given by

$$\frac{L}{E} \lesssim 10^4 \,\mathrm{km/GeV} \quad \Longrightarrow \quad \Delta m^2 \gtrsim 10^{-4} \,\mathrm{eV}^2 \,. \tag{7.91}$$

These experiments are under study; new and more intense neutrino beams are needed in order to observe a sufficient number of events at such large distances. Candidate types of beam are: Super-Beam [552], Beta-Beam [1091, 796, 59, 576], and Neutrino Factory [511, 58, 99, 59, 576].

SOLar neutrino experiments (SOL). These are experiments which detect the neutrinos generated in the core of the Sun by the thermonuclear reactions that power the Sun. The Sun–Earth distance is about 1.5×10^{11} m. Since the energy

of detectable solar neutrinos is in the range 0.2–15 MeV, the range of L/E and the sensitivity to Δm^2 in solar neutrino experiments are

$$\frac{L}{E} \lesssim 10^{12}\,\mathrm{m/MeV} \quad \Longrightarrow \quad \Delta m^2 \gtrsim 10^{-12}\,\mathrm{eV}^2\,. \tag{7.92}$$

Hence, solar neutrino experiments are sensitive to extremely small values of Δm^2, much smaller than the sensitivity of the other experiment discussed above. Several solar neutrino experiments have been performed in the past: Homestake [323], Kamiokande [475], GALLEX [588], SAGE [19], GNO [76], SNO [45]. The SNO experiment is still in operation. In the future, the Borexino [1008] experiment, which is under construction, will start data taking and the KamLAND experiments may be improved to detect solar neutrinos [399]. Several other experiments are under study (see Ref. [938]).

The types of neutrino oscillation experiments with their typical source–detector distance, energy, and sensitivity to Δm^2 are summarized in Table 7.1.

7.6 Averaged transition probability

In practice, it is impossible to measure the oscillation probabilities for precise values of the neutrino propagation distance L and the neutrino energy E, because in any experiment both the source and the detection processes have some spatial uncertainty, i.e. the source has an energy spectrum and the energy resolution of the detector is finite. Therefore, in practice it is always necessary to average the oscillation probability over the appropriate distributions of the distance L and the energy E.

Considering the simplest case of two-neutrino mixing, the transition probability measured in practice is obtained by averaging the cosine function in eqn (7.69) over the appropriate distribution $\phi(L/E)$ of L/E:

$$\langle P_{\nu_\alpha \to \nu_\beta}(L,E)\rangle = \frac{1}{2}\,\sin^2 2\vartheta \left[1 - \left\langle \cos\!\left(\frac{\Delta m^2 L}{2E}\right)\right\rangle\right] \qquad (\alpha \neq \beta)\,, \tag{7.93}$$

with

$$\left\langle \cos\!\left(\frac{\Delta m^2 L}{2E}\right)\right\rangle = \int \cos\!\left(\frac{\Delta m^2 L}{2E}\right) \phi\!\left(\frac{L}{E}\right)\,\mathrm{d}\frac{L}{E}\,. \tag{7.94}$$

In order to illustrate the effect of these averages, let us consider the simplest case of a Gaussian L/E distribution with average $\langle L/E\rangle$ and standard deviation $\sigma_{L/E}$:

$$\phi\!\left(\frac{L}{E}\right) = \frac{1}{\sqrt{2\pi\sigma_{L/E}^2}}\,\exp\left[\frac{(L/E - \langle L/E\rangle)^2}{2\,\sigma_{L/E}^2}\right]\,. \tag{7.95}$$

In this case, the average of the cosine in eqn (7.93) can be calculated analytically, yielding

$$\left\langle \cos\!\left(\frac{\Delta m^2 L}{2E}\right)\right\rangle = \cos\!\left(\frac{\Delta m^2}{2}\,\left\langle\frac{L}{E}\right\rangle\right) \exp\left[-\frac{1}{2}\left(\frac{\Delta m^2}{2}\,\sigma_{L/E}\right)^2\right]\,. \tag{7.96}$$

The solid line in Fig. 7.2 shows the corresponding averaged transition probability as a function of $\langle L/E\rangle\,[\mathrm{km/GeV}]\,\Delta m^2\,[\mathrm{eV}^2]$ for $\sin^2 2\vartheta = 1$ and $\sigma_{L/E} = 0.2\,\langle L/E\rangle$. It is reasonable to assume an uncertainty $\sigma_{L/E}$ proportional to $\langle L/E\rangle$. Since the uncertainties of L and E are independent, we have

$$\left(\frac{\sigma_{L/E}}{\langle L/E\rangle}\right)^2 = \left(\frac{\sigma_L}{\langle L\rangle}\right)^2 + \left(\frac{\sigma_E}{\langle E\rangle}\right)^2 , \tag{7.97}$$

where $\langle L\rangle$ is the average distance, σ_L is the distance uncertainty, $\langle E\rangle$ is the average energy, and σ_E is the energy uncertainty.

For fixed values of the squared-mass difference Δm^2 and of the average energy $\langle E\rangle$, the horizontal axis in Fig. 7.2 is approximately proportional to the average distance $\langle L\rangle$ and the solid curve represents the behavior of the transition probability in eqn (7.70) as a function of $\langle L\rangle$. One can see that for distances $\langle L\rangle \lesssim L^{\mathrm{osc}}$, which corresponds to $\langle L/E\rangle\,[\mathrm{km/GeV}]\,\Delta m^2\,[\mathrm{eV}^2] = 2.47$, the averaged transition probability oscillates as the unaveraged transition probability given by the dashed line, with amplitude somewhat suppressed, the suppression being dependent on the width $\sigma_{L/E}$ of the energy distribution (a larger width gives more suppression). For distances $\langle L\rangle \gg L^{\mathrm{osc}}$, the oscillations are completely suppressed and one can measure only the average transition probability in eqn (7.73).

If an oscillation experiment does not observe any oscillation, the data imply an upper limit on the averaged transition probability:

$$\langle P_{\nu_\alpha\to\nu_\beta}(L,E)\rangle \leq P^{\max}_{\nu_\alpha\to\nu_\beta} , \tag{7.98}$$

which implies an upper limit for $\sin^2 2\vartheta$ as a function of Δm^2: considering the averaged transition probability in eqn (7.93) we have

$$\sin^2 2\vartheta \leq \frac{2\,P^{\max}_{\nu_\alpha\to\nu_\beta}}{1 - \left\langle \cos\left(\dfrac{\Delta m^2 L}{2E}\right)\right\rangle} . \tag{7.99}$$

The solid line in Fig. 7.3a shows this upper limit as a function of $\Delta m^2\,[\mathrm{eV}^2]\,\langle L/E\rangle\,[\mathrm{km/GeV}]$ for $P^{\max}_{\nu_\alpha\to\nu_\beta} = 0.1$, and the Gaussian energy distribution in eqn (7.95) with $\sigma_{L/E} = 0.2\,\langle L/E\rangle$ (the dashed line shows the upper limit corresponding to the unaveraged transition probability, i.e. $\sigma_{L/E} = 0$). The solid line in Fig. 7.3a is usually called the *exclusion curve*, because it separates the allowed region from the indicated excluded region. From Fig. 7.3a one can see that there is no limit on $\sin^2 2\vartheta$ for

$$\frac{\Delta m^2}{2}\left\langle\frac{L}{E}\right\rangle \ll \pi \quad\Longleftrightarrow\quad \Delta m^2\,[\mathrm{eV}^2]\left\langle\frac{L}{E}\right\rangle\frac{[\mathrm{km}]}{[\mathrm{GeV}]} \ll 1 . \tag{7.100}$$

The reason is that in this case the cosine function in eqn (7.99) is practically constant and equal to unity in the range of L/E relevant for the integration. This is true when the variance of L/E is always much smaller than the square of the

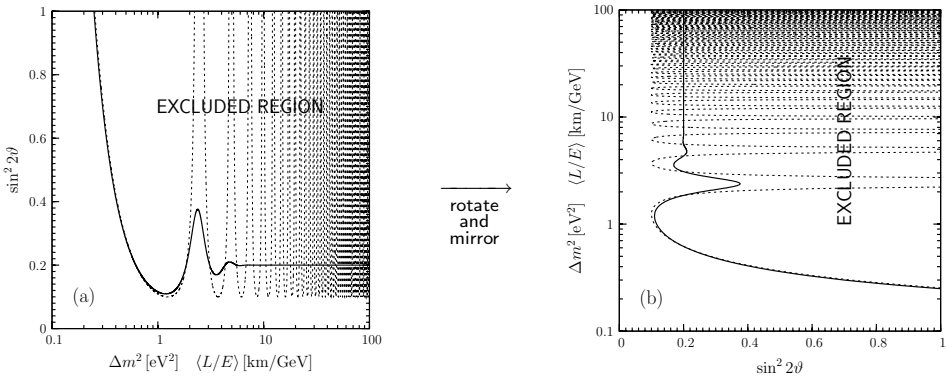

FIG. 7.3. Upper limit in eqn (7.99) with a Gaussian L/E distribution as a function of $\Delta m^2\,[\mathrm{eV}^2]\,\langle L/E\rangle\,[\mathrm{km/GeV}]$ for $P^{\max}_{\nu_\alpha\to\nu_\beta} = 0.1$. Solid line: $\sigma_{L/E} = 0.2\,\langle L/E\rangle$. Dashed line: $\sigma_{L/E} = 0$, which corresponds to $P_{\nu_\alpha\to\nu_\beta}(L,E) \leq P^{\max}_{\nu_\alpha\to\nu_\beta}$ with $L/E = \langle L/E\rangle$, where $P_{\nu_\alpha\to\nu_\beta}(L,E)$ is the unaveraged transition probability in eqn (7.70).

average value,

$$\left\langle \left(\frac{L}{E} - \left\langle \frac{L}{E} \right\rangle \right)^2 \right\rangle = \left\langle \left(\frac{L}{E} \right)^2 \right\rangle - \left(\left\langle \frac{L}{E} \right\rangle \right)^2 \ll \left(\left\langle \frac{L}{E} \right\rangle \right)^2 , \tag{7.101}$$

which is the case in real experiments.

The most stringent bound on $\sin^2 2\vartheta$ is obtained for

$$\frac{\Delta m^2}{2} \left\langle \frac{L}{E} \right\rangle \simeq \pi \quad \Longleftrightarrow \quad \Delta m^2\,[\mathrm{eV}^2] \left\langle \frac{L}{E} \right\rangle \frac{[\mathrm{km}]}{[\mathrm{GeV}]} \simeq 1.24\,. \tag{7.102}$$

In this case, the cosine function in eqn (7.99) is approximately equal to -1 over the relevant range of L/E.

For much larger values of Δm^2, the limit on $\sin^2 2\vartheta$ does not depend on Δm^2:

$$\sin^2 2\vartheta \leq 2\, P^{\max}_{\nu_\alpha\to\nu_\beta}\,, \tag{7.103}$$

for

$$\frac{\Delta m^2}{2} \left\langle \frac{L}{E} \right\rangle \gg \pi \quad \Longleftrightarrow \quad \Delta m^2\,[\mathrm{eV}^2] \left\langle \frac{L}{E} \right\rangle \frac{[\mathrm{km}]}{[\mathrm{GeV}]} \gg 1\,. \tag{7.104}$$

In this case, the argument of the cosine function in eqn (7.99) is very large and rapidly oscillating in the relevant range of L/E, leading to a vanishing average.

Let us examine more closely the inequality in eqn (7.99) for small values of $\Delta m^2\,\langle L/E\rangle$. From eqn (7.101), if $\Delta m^2\,\langle L/E\rangle \ll 2\pi$, the argument of the cosine function in eqn (7.99) becomes small in the relevant range of L/E and the cosine

function can be approximated by

$$\cos\left(\frac{\Delta m^2 L}{2E}\right) \simeq 1 - \frac{1}{2}\left(\frac{\Delta m^2 L}{2E}\right)^2 . \tag{7.105}$$

This approximation allows one to write the bound in eqn (7.99) as

$$\sin^2 2\vartheta \lesssim \frac{2\, P^{\max}_{\nu_\alpha \to \nu_\beta}}{\frac{1}{2}\left(\frac{\Delta m^2}{2}\right)^2 \left\langle \left(\frac{L}{E}\right)^2 \right\rangle} . \tag{7.106}$$

Because of eqn (7.101), we can approximate $\langle (L/E)^2 \rangle$ with $(\langle L/E \rangle)^2$ and obtain

$$\sin^2 2\vartheta \lesssim \frac{2\, P^{\max}_{\nu_\alpha \to \nu_\beta}}{\frac{1}{2}\left(\frac{\Delta m^2}{2}\left\langle \frac{L}{E} \right\rangle\right)^2} \quad \Longleftrightarrow \quad \sin^2 2\vartheta \lesssim \frac{0.62\, P^{\max}_{\nu_\alpha \to \nu_\beta}}{\left(\Delta m^2\,[\mathrm{eV}^2]\left\langle \frac{L}{E} \right\rangle \frac{[\mathrm{km}]}{[\mathrm{GeV}]}\right)^2} . \tag{7.107}$$

The right-hand side of this inequality is a quadratic function of Δm^2, which appears as the straight-line part of the exclusion curve for small $\Delta m^2\,[\mathrm{eV}^2]\,\langle L/E \rangle\,[\mathrm{km/GeV}]$ in Fig. 7.3a, due to the logarithmic scale. The intercept of the exclusion curve with the $\sin^2 2\vartheta = 1$ axis occurs at

$$\frac{\Delta m^2}{2}\left\langle \frac{L}{E} \right\rangle \simeq 2\sqrt{P^{\max}_{\nu_\alpha \to \nu_\beta}} \quad \Longleftrightarrow \quad \Delta m^2\,[\mathrm{eV}^2]\left\langle \frac{L}{E} \right\rangle \frac{[\mathrm{km}]}{[\mathrm{GeV}]} \simeq 0.79\sqrt{P^{\max}_{\nu_\alpha \to \nu_\beta}} . \tag{7.108}$$

For example, one can see in Fig. 7.3a, which has been drawn for $\sqrt{P^{\max}_{\nu_\alpha \to \nu_\beta}} = 0.32$, that the intercept of the exclusion curve with the $\sin^2 2\vartheta = 1$ axis occurs at $\Delta m^2\,[\mathrm{eV}^2]\,\langle L/E \rangle\,[\mathrm{km/GeV}] \simeq 0.25$.

The experimental bound on $\sin^2 2\vartheta$ as a function of Δm^2 is usually presented by rotating and mirroring Fig. 7.3a, as shown in Fig. 7.3b, with $\sin^2 2\vartheta$ on the horizontal axis and Δm^2, for a fixed value of $\langle L/E \rangle$, on the vertical axis. In these figures which are called the *exclusion plots*, the excluded region of the oscillation parameters $\sin^2 2\vartheta$ and Δm^2 always lies on the right of the exclusion curve. Figure 7.4a shows an example of an exclusion curve obtained for $P^{\max}_{\nu_\alpha \to \nu_\beta} = 0.1$ and a Gaussian L/E distribution with $\langle L/E \rangle = 1\,\mathrm{km/GeV}$ and $\sigma_{L/E} = 0.2\,\mathrm{km/GeV}$.

In some disappearance experiments, the initial neutrino flux is not well known. In such a case, if the shape of the initial energy spectrum is known, information on transitions in different flavors can be obtained by measuring the distortions of the spectrum. Obviously, in this case one cannot obtain any information on oscillations if $\Delta m^2 \langle L/E \rangle \gg 2\pi$, because, as shown in Fig. 7.2 and eqn (7.103), the averaged transition probability is independent of energy. A similar situation is realized in experiments in which a *near* detector is placed upstream of the neutrino beam in order to measure the neutrino flux, whereas disappearance of the original neutrino flavor is measured at a *far* detector. No information on oscillations can be obtained if $\Delta m^2 \langle L/E \rangle_{\mathrm{near}} \gtrsim 2\pi$, because in this case the near detector already measures the averaged oscillated neutrino flux.

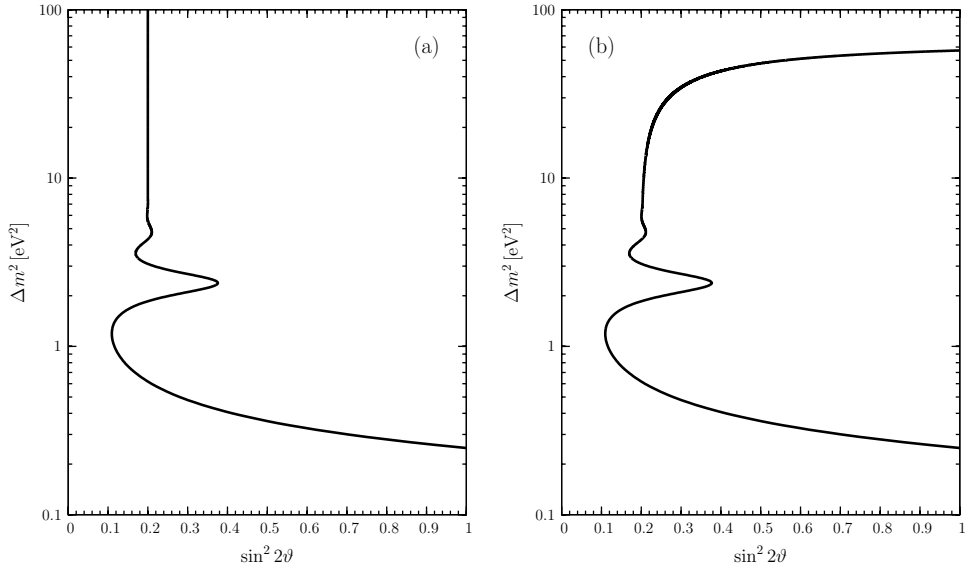

FIG. 7.4. Examples of exclusion plots in the plane of the two-neutrino oscillation parameters $\sin^2 2\vartheta$ and Δm^2. (a) Example of an exclusion plot obtained for $P^{\max}_{\nu_\alpha \to \nu_\beta} = 0.1$ and a Gaussian L/E distribution with $\langle L/E \rangle = 1\,\text{km/GeV}$ and $\sigma_{L/E} = 0.2\,\text{km/GeV}$. (b) Example of an exclusion plot that could be obtained in a disappearance experiment with two detectors using eqn (7.111) with $R = 0.9$ and a Gaussian L/E distribution with $\langle L/E \rangle_{\text{near}} = 0.01\,\text{km/GeV}$, $\sigma^{\text{near}}_{L/E} = 0.002\,\text{km/GeV}$ and $\langle L/E \rangle_{\text{far}} = 1\,\text{km/GeV}$, $\sigma^{\text{far}}_{L/E} = 0.2\,\text{km/GeV}$.

As an example, let us consider a disappearance experiment with two detectors which measure

$$\frac{\langle P_{\nu_\alpha \to \nu_\alpha}(L,E) \rangle_{\text{far}}}{\langle P_{\nu_\alpha \to \nu_\alpha}(L,E) \rangle_{\text{near}}} \geq R\,, \tag{7.109}$$

where $0 \leq R < 1$. The inequality in eqn (7.109) means that the experiment did not find any indication of flavor transitions, which then yields an exclusion curve in the $\sin^2 2\vartheta$-Δm^2 plane. Since the averaged survival probability is given by

$$\langle P_{\nu_\alpha \to \nu_\alpha}(L,E) \rangle = 1 - \frac{1}{2} \sin^2 2\vartheta \left[1 - \left\langle \cos\left(\frac{\Delta m^2 L}{2E} \right) \right\rangle \right], \tag{7.110}$$

the inequality in eqn (7.109) can be written as

$$\sin^2 2\vartheta \leq 2 \left[1 - (1-R)^{-1} \left(\left\langle \cos\left(\frac{\Delta m^2 L}{2E} \right) \right\rangle_{\text{far}} - R \left\langle \cos\left(\frac{\Delta m^2 L}{2E} \right) \right\rangle_{\text{near}} \right) \right]^{-1}. \tag{7.111}$$

Figure 7.4b shows the exclusion curve obtained with eqn (7.111) for $R = 0.9$ and a Gaussian L/E distribution with $\langle L/E \rangle_{\text{near}} = 0.01\,\text{km/GeV}$, $\sigma^{\text{near}}_{L/E} = 0.002\,\text{km/GeV}$ and $\langle L/E \rangle_{\text{far}} = 1\,\text{km/GeV}$, $\sigma^{\text{far}}_{L/E} = 0.2\,\text{km/GeV}$. One can see that there is no limit

on $\sin^2 2\vartheta$ for $\Delta m^2 \gtrsim 60\,\mathrm{eV}^2$, which corresponds to $\Delta m^2 \langle L/E \rangle_{\mathrm{near}} \gtrsim 3$. For such large values of Δm^2, oscillations occur between the source and the near detector, preventing a measurement of the initial neutrino flux.

If an experiment detects a positive signal, the flavor transition probability is limited in a range which corresponds to an allowed band in the $\sin^2 2\vartheta$-Δm^2 plane, as shown in the example in Fig. 7.5a, obtained for $0.05 \leq \langle P_{\nu_\alpha \to \nu_\beta} \rangle \leq 0.15$ and a Gaussian L/E distribution with $\langle L/E \rangle = 1\,\mathrm{km/GeV}$ and $\sigma_{L/E} = 0.15\,\mathrm{km/GeV}$. However, in most experiments the position and energy of each event is measured, with some uncertainty. Therefore, there is not only one global L/E distribution, but typically the data are binned and each bin has its own L/E distribution. The allowed bands of the different bins are combined in a statistical analysis that typically yields one or more allowed regions in the $\sin^2 2\vartheta$-Δm^2 plane. The effect of combining the results of different L/E distributions is illustrated by Fig. 7.5b, where we have plotted two curves obtained with Gaussian L/E distributions, corresponding to $\langle P_{\nu_\alpha \to \nu_\beta} \rangle = 0.11$, $\langle L/E \rangle = 2\,\mathrm{km/GeV}$, $\sigma_{L/E} = 0.25\,\mathrm{km/GeV}$ and $\langle P_{\nu_\alpha \to \nu_\beta} \rangle = 0.09$, $\langle L/E \rangle = 0.4\,\mathrm{km/GeV}$, $\sigma_{L/E} = 0.05\,\mathrm{km/GeV}$. One can see that the two curves overlap at several points in the $\sin^2 2\vartheta$-Δm^2 plane. These points are compatible with both $\langle P_{\nu_\alpha \to \nu_\beta} \rangle$'s. If the uncertainties of the two $\langle P_{\nu_\alpha \to \nu_\beta} \rangle$'s are taken into account, a combined fit would yield allowed regions around the points of overlap of the two curves. It is clear that adding more information, i.e. more measurements of $P_{\nu_\alpha \to \nu_\beta}$ at different values of $\langle L/E \rangle$, results in fewer points of overlap of the corresponding curves and a smaller number of allowed regions in the $\sin^2 2\vartheta$-Δm^2 plane. The final experimental goal is, of course, to select only one, possibly small, allowed region in the $\sin^2 2\vartheta$-Δm^2 plane.

So far we have considered averaged oscillations only in the simplest case of two-neutrino mixing. In a general case of mixing of any number of neutrinos, the average of the oscillation probability in eqn (7.37) over an appropriate distribution $\phi(L/E)$ of L/E is given by

$$\langle P_{\nu_\alpha \to \nu_\beta}(L,E) \rangle = \delta_{\alpha\beta} - 2 \sum_{k>j} \Re\mathfrak{e} \left[U^*_{\alpha k}\, U_{\beta k}\, U_{\alpha j}\, U^*_{\beta j} \right] \left[1 - \left\langle \cos\left(\frac{\Delta m^2_{kj} L}{2E} \right) \right\rangle \right] + 2 \sum_{k>j} \Im\mathfrak{m} \left[U^*_{\alpha k}\, U_{\beta k}\, U_{\alpha j}\, U^*_{\beta j} \right] \left\langle \sin\left(\frac{\Delta m^2_{kj} L}{2E} \right) \right\rangle . \quad (7.112)$$

In the case of a Gaussian L/E distribution, the averaged cosine is given by eqn (7.96) and the averaged sine is given by

$$\left\langle \sin\left(\frac{\Delta m^2_{kj} L}{2E} \right) \right\rangle = \sin\left(\frac{\Delta m^2}{2} \left\langle \frac{L}{E} \right\rangle \right) \exp\left[-\frac{1}{2} \left(\frac{\Delta m^2}{2}\, \sigma_{L/E} \right)^2 \right] . \quad (7.113)$$

It is clear that, in general, the expression in eqn (7.112) is a complicated function of several parameters (squared mass differences, mixing angles, and CP phases).

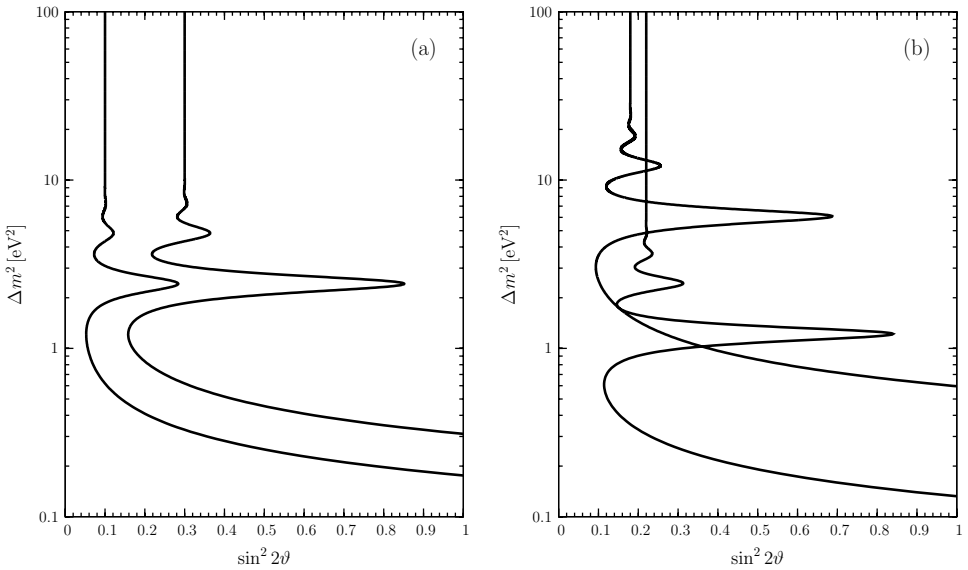

FIG. 7.5. Examples of plots in the plane of the two-neutrino oscillation parameters $\sin^2 2\vartheta$ and Δm^2. (a) Example of an allowed region, between the two curves, obtained for $0.05 \leq P_{\nu_\alpha \to \nu_\beta} \leq 0.15$ and a Gaussian L/E distribution with $\langle L/E \rangle = 1\,\text{km/GeV}$ and $\sigma_{L/E} = 0.15\,\text{km/GeV}$. (b) Example of two best-fit curves obtained with a Gaussian L/E distribution; the curve which reaches lower values of Δm^2 corresponds to $P_{\nu_\alpha \to \nu_\beta} = 0.11$, $\langle L/E \rangle = 2\,\text{km/GeV}$, and $\sigma_{L/E} = 0.25\,\text{km/GeV}$; the other curve, which reaches lower values of $\sin^2 2\vartheta$ for large Δm^2, corresponds to $P_{\nu_\alpha \to \nu_\beta} = 0.09$, $\langle L/E \rangle = 0.4\,\text{km/GeV}$, and $\sigma_{L/E} = 0.05\,\text{km/GeV}$.

7.7 Large Δm^2 dominance

In this section we consider the case in which one scale of neutrino squared-mass differences is much larger than the others. This means that the massive neutrinos can be divided in two groups, which we call A and B, such that all the squared-mass differences between two neutrinos belonging to different groups are much larger than all the squared-mass differences between two neutrinos belonging to one of the two groups, as illustrated schematically in Fig. 7.6.

This type of schemes is realized, for example, in the case of three-neutrino mixing with a hierarchy of Δm^2's (see Fig. 13.1 on page 453).

Let us denote with N_A and N_B the numbers of massive neutrinos belonging, respectively, to A and B, with the total number of massive neutrinos equal to $N = N_A + N_B$. We assign the numbers of the massive neutrinos in such a way that $\nu_1, \ldots, \nu_{N_A} \in A$ and $\nu_{N_A+1}, \ldots, \nu_N \in B$. Then, there is dominance of the largest Δm^2 if

$$|\Delta m^2_{N1}| \gg |\Delta m^2_{kj}| \quad \text{for} \quad k, j \leq N_A \quad \text{or} \quad k, j > N_A \,. \tag{7.114}$$

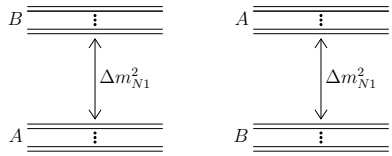

FIG. 7.6. Schematic illustration of the two possible types of neutrino mass spectra with a dominant scale of squared-mass difference. The dots indicate possible massive neutrinos with squared-mass differences much smaller than $|\Delta m^2_{N1}|$.

In this case

$$|\Delta m^2_{kj}| \simeq |\Delta m^2_{N1}| \quad \text{for} \quad (k \leq N_A \text{ and } j > N_A) \quad \text{or} \quad (k > N_A \text{ and } j \leq N_A)\,. \tag{7.115}$$

Hence, Δm^2_{N1} is the dominant squared-mass difference.

Let us consider an experiment which is sensitive to oscillations generated by the dominant squared-mass difference Δm^2_{N1}. This means that

$$\frac{|\Delta m^2_{N1}|}{2} \left\langle \frac{L}{E} \right\rangle \sim \pi\,, \tag{7.116}$$

and

$$\frac{|\Delta m^2_{kj}|}{2} \left\langle \frac{L}{E} \right\rangle \ll \pi \quad \text{for} \quad k, j \leq N_A \quad \text{or} \quad k, j > N_A\,. \tag{7.117}$$

In this case, the oscillation probability in eqn (7.23),

$$P_{\nu_\alpha \to \nu_\beta}(L, E) = \left| \sum_k U^*_{\alpha k}\, U_{\beta k}\, \exp\left(-i\, \frac{\Delta m^2_{k1} L}{2E}\right) \right|^2\,, \tag{7.118}$$

can be separated into the contributions with $k \leq N_A$ and those with $k > N_A$,

$$P_{\nu_\alpha \to \nu_\beta}(L, E) = \left| \sum_{k \leq N_A} U^*_{\alpha k}\, U_{\beta k}\, \exp\left(-i\, \frac{\Delta m^2_{k1} L}{2E}\right) + \sum_{k > N_A} U^*_{\alpha k}\, U_{\beta k}\, \exp\left(-i\, \frac{\Delta m^2_{k1} L}{2E}\right) \right|^2\,. \tag{7.119}$$

Because of eqns (7.116) and (7.117), we can neglect the phases of the first group and we can approximate all the phases of the second group with $\Delta m^2_{N1} L/2E$, leading to the effective probability

$$P^{\text{eff}}_{\nu_\alpha \to \nu_\beta}(L, E) = \left| \sum_{k \leq N_A} U^*_{\alpha k}\, U_{\beta k} + \exp\left(-i\, \frac{\Delta m^2_{N1} L}{2E}\right) \sum_{k > N_A} U^*_{\alpha k}\, U_{\beta k} \right|^2\,. \tag{7.120}$$

Using the unitarity relation in eqn (7.28), the above probability can be written as

$$P^{\rm eff}_{\nu_\alpha\to\nu_\beta}(L,E) = \left|\delta_{\alpha\beta} - \left[1 - \exp\left(-i\,\frac{\Delta m^2_{N1} L}{2E}\right)\right] \widetilde{\sum_k} U^*_{\alpha k}\, U_{\beta k}\right|^2 , \qquad (7.121)$$

where the symbol $\widetilde{\sum}_k$ indicates a sum over the index k that can be performed either over the range $1\,,\,\ldots\,,\,N_A$ or over the range $N_A+1\,,\,\ldots\,,\,N$:

$$\widetilde{\sum_k} U^*_{\alpha k}\, U_{\beta k} = \sum_{k\le N_A} U^*_{\alpha k}\, U_{\beta k} \qquad \text{or} \qquad \widetilde{\sum_k} U^*_{\alpha k}\, U_{\beta k} = \sum_{k> N_A} U^*_{\alpha k}\, U_{\beta k}\,. \qquad (7.122)$$

The squared modulus in eqn (7.121) is easily evaluated, yielding

$$P^{\rm eff}_{\nu_\alpha\to\nu_\beta}(L,E) = \delta_{\alpha\beta} - 4\left[\delta_{\alpha\beta}\widetilde{\sum_k}|U^*_{\alpha k}|^2 - \left|\widetilde{\sum_k} U^*_{\alpha k}\, U_{\beta k}\right|^2\right] \sin^2\left(\frac{\Delta m^2_{N1} L}{4E}\right) . \qquad (7.123)$$

For the transition probabilities we have

$$P^{\rm eff}_{\nu_\alpha\to\nu_\beta}(L,E) = 4\left|\widetilde{\sum_k} U^*_{\alpha k}\, U_{\beta k}\right|^2 \sin^2\left(\frac{\Delta m^2_{N1} L}{4E}\right) \qquad (\alpha\neq\beta)\,. \qquad (7.124)$$

Comparing with eqn (7.70), we see that the transition probability in eqn (7.124) corresponds to an effective two-neutrino-like transition probability,

$$P^{\rm eff}_{\nu_\alpha\to\nu_\beta}(L,E) = \sin^2 2\vartheta^{\rm eff}_{\alpha\beta}\, \sin^2\left(\frac{\Delta m^2_{N1} L}{4E}\right) \qquad (\alpha\neq\beta)\,, \qquad (7.125)$$

with effective squared-mass difference Δm^2_{N1} and effective mixing angle $\vartheta^{\rm eff}_{\alpha\beta}$ given by

$$\sin^2 2\vartheta^{\rm eff}_{\alpha\beta} = 4\left|\widetilde{\sum_k} U^*_{\alpha k}\, U_{\beta k}\right|^2 . \qquad (7.126)$$

This definition of an effective mixing angle is consistent, because using the Cauchy–Schwartz inequality on the two equivalent expressions in eqn (7.122) we have

$$\left|\widetilde{\sum_k} U^*_{\alpha k}\, U_{\beta k}\right|^2 \le \left(\sum_{k\le N_A}|U_{\alpha k}|^2\right)\left(\sum_{k\le N_A}|U_{\beta k}|^2\right) \qquad (7.127)$$

and

$$\begin{aligned}\left|\widetilde{\sum_k} U^*_{\alpha k}\, U_{\beta k}\right|^2 &\le \left(\sum_{k> N_A}|U_{\alpha k}|^2\right)\left(\sum_{k> N_A}|U_{\beta k}|^2\right) \\ &= \left(1 - \sum_{k\le N_A}|U_{\alpha k}|^2\right)\left(1 - \sum_{k\le N_A}|U_{\beta k}|^2\right) . \qquad (7.128)\end{aligned}$$

Hence, the maximum of $\left|\widetilde{\sum}_k U^*_{\alpha k} U_{\beta k}\right|^2$ is 1/4, reached for $\sum_{k\leq N_A} |U_{\alpha k}|^2 = \sum_{k\leq N_A} |U_{\beta k}|^2 = 1/2$. The definition in eqn (7.126) corresponds to two possible values of the effective mixing angle symmetric with respect to $\pi/4$, which are given by

$$\sin\vartheta^{\rm eff}_{\alpha\beta} = \frac{1}{\sqrt{2}}\left(1 \pm \sqrt{1 - 4\left|\widetilde{\sum_k} U^*_{\alpha k} U_{\beta k}\right|^2}\right)^{1/2} . \tag{7.129}$$

The effective transition probability in eqn (7.125) is very useful for the analysis of experimental data of appearance experiments which satisfy the conditions in eqns (7.116) and (7.117), since it implies that the two effective parameters are sufficient for the description of the data.

It is interesting to note that, although the effective mixing angle in eqn (7.129) may depend on the Dirac phases in the mixing matrix, it is invariant under CP or T transformation, which correspond to a charge conjugation of the elements of the mixing matrix. Hence, the effective mixing angle can depend only on the cosines of the Dirac phases in the mixing matrix. Its invariance under CP and T transformation implies that

$$P^{\rm eff}_{\nu_\alpha\to\nu_\beta} = P^{\rm eff}_{\bar\nu_\alpha\to\bar\nu_\beta} = P^{\rm eff}_{\bar\nu_\beta\to\bar\nu_\alpha} = P^{\rm eff}_{\nu_\beta\to\nu_\alpha} , \tag{7.130}$$

i.e. all the CP and T asymmetries are zero:

$$A^{\rm T}_{\alpha\beta} = -\bar A^{\rm T}_{\alpha\beta} = A^{\rm CP}_{\alpha\beta} = 0 . \tag{7.131}$$

Therefore, an experiment which is sensitive only to the largest squared-mass difference cannot probe CP violations.

From eqn (7.121), the survival probabilities in the case of large Δm^2 dominance are given by

$$P^{\rm eff}_{\nu_\alpha\to\nu_\alpha}(L,E) = 1 - 4\left(\widetilde{\sum_k}|U_{\alpha k}|^2\right)\left(1 - \widetilde{\sum_k}|U_{\alpha k}|^2\right)\sin^2\left(\frac{\Delta m^2_{N1}L}{4E}\right) . \tag{7.132}$$

Comparing with eqn (7.71), one can see that the survival probability in eqn (7.132) corresponds to an effective two-neutrino-like survival probability,

$$P^{\rm eff}_{\nu_\alpha\to\nu_\alpha}(L,E) = 1 - \sin^2 2\vartheta^{\rm eff}_{\alpha\alpha}\,\sin^2\left(\frac{\Delta m^2_{N1}L}{4E}\right) , \tag{7.133}$$

with an effective squared-mass difference Δm^2_{N1} and an effective mixing angle $\vartheta^{\rm eff}_{\alpha\alpha}$ given by

$$\sin^2 2\vartheta^{\rm eff}_{\alpha\alpha} = 4\left(\widetilde{\sum_k}|U_{\alpha k}|^2\right)\left(1 - \widetilde{\sum_k}|U_{\alpha k}|^2\right) . \tag{7.134}$$

This definition of an effective mixing angle makes sense, since the upper bound of the right-hand side is one, which is reached for $\widetilde{\sum}_k |U_{\alpha k}|^2 = \frac{1}{2}$. Equation (7.134)

corresponds to two possible values of the effective mixing angle symmetric with respect to $\pi/4$, which are given by

$$\sin\vartheta^{\rm eff}_{\alpha\alpha} = \widetilde{\sum_k} |U_{\alpha k}|^2 \quad \text{or} \quad \sin\vartheta^{\rm eff}_{\alpha\alpha} = 1 - \widetilde{\sum_k} |U_{\alpha k}|^2 \,. \tag{7.135}$$

The effective survival probability in eqn (7.125), which depends only on two parameters, is very useful for the analysis of experimental data of disappearance experiments in which the conditions in eqns (7.116) and (7.117) are satisfied.

The effective two-neutrino-like oscillation probabilities averaged over the appropriate distributions of the distance L and the energy E have the same properties as the averaged oscillations in two-neutrino mixing discussed in section 7.6.

Let us emphasize that from a theoretical point of view the large Δm^2 dominance is a realistic possibility. The simplest and most plausible case in which it is realized is through a hierarchy of squared-mass differences, which could be due to a hierarchy of neutrino masses. If there is a hierarchy of squared-mass differences, there is only one squared-mass which is much larger than the others, leading to a considerable simplification of the expressions of the effective mixing angles in eqns (7.126) and (7.134):

$$\sin^2 2\vartheta^{\rm eff}_{\alpha\beta} = 4\,|U_{\alpha N}|^2\,|U_{\beta N}|^2 \quad (\alpha \neq \beta)\,, \qquad \sin^2 2\vartheta^{\rm eff}_{\alpha\alpha} = 4\,|U_{\alpha N}|^2\left(1 - |U_{\alpha N}|^2\right)\,. \tag{7.136}$$

We will see in chapter 13 that the results of neutrino oscillation experiments show that the neutrino spectrum has a hierarchy of squared-mass differences and the effective mixing angles in eqn (7.136) can be applied with success to the analysis of the data of experiments which are sensitive only to the largest Δm^2. The relations in eqn (7.131) imply that these experiments cannot measure CP or T violations.

7.8 Active small Δm^2

In this section we discuss a case in which there is a scale of neutrino squared-mass differences which is much smaller than the largest scale of squared-mass differences. We derive the effective oscillation probabilities in experiments which are sensitive to such a small Δm^2. In these experiments the small Δm^2 under consideration is *active*, because it generates the measurable oscillations which depend on L and E. It is possible that in addition to the largest squared-mass difference there are also squared-mass differences much smaller than the active one. Therefore, we consider a general case in which the massive neutrinos can be divided in three groups that we call A_1, A_2, and B, with the following properties. All the squared-mass differences between a neutrino belonging to A_1 and a neutrino belonging to A_2 are much larger than all the squared-mass differences between two neutrinos belonging either to A_1 or to A_2 or to B. Moreover, all the squared-mass differences between a neutrino belonging to A_1 and a neutrino belonging to A_2 are much smaller than all the squared-mass differences between a neutrino belonging to A_1 or A_2 and a neutrino belonging to B. These properties are illustrated schematically in Fig. 7.7. A more general case in which there can also be squared-mass differences between two

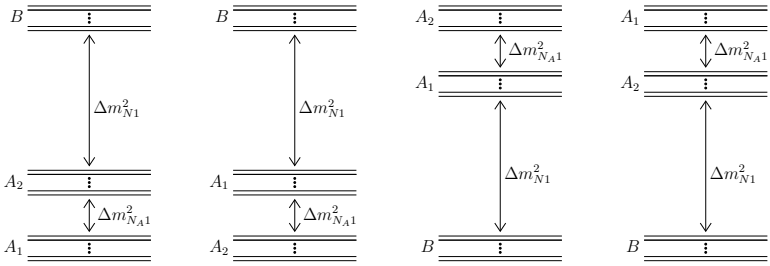

FIG. 7.7. Schematic illustration of the four possible types of neutrino mass spectra considered in section 7.8. The dots indicate possible massive neutrinos with squared-mass differences much smaller than $|\Delta m^2_{N_A1}|$.

neutrinos belonging to B which are much larger than the squared-mass differences between a neutrino belonging to A_1 and a neutrino belonging to A_2 can also be treated, but we avoid it because the formalism becomes too cumbersome.

The general case discussed in this section is useful in practice, for example, in the study of neutrino oscillations in vacuum due to Δm^2_{21} in a three-neutrino mixing scheme with a hierarchy of Δm^2's, as explained in section 13.1.2.

Let us denote by N_{A_1}, N_{A_2}, and N_B the numbers of massive neutrinos belonging, respectively, to A_1, A_2, and B, with the total number of massive neutrinos equal to $N = N_{A_1} + N_{A_2} + N_B$. It is also convenient to call $A = A_1 \cup A_2$ and denote with N_A the number of massive neutrinos belonging to A ($N_A = N_{A_1} + N_{A_2}$). Let us assign the numbers of the massive neutrinos in such a way that $\nu_1, \ldots, \nu_{N_{A_1}} \in A_1$, $\nu_{N_{A_1}+1}, \ldots, \nu_{N_A} \in A_2$ and $\nu_{N_A+1}, \ldots, \nu_N \in B$. We consider a neutrino mass spectrum such that

$$|\Delta m^2_{N_A1}| \gg |\Delta m^2_{kj}| \quad \text{for} \quad \left\{ \begin{array}{c} k, j \leq N_{A_1} \\ \text{or} \\ N_{A_1} < k, j \leq N_A \\ \text{or} \\ k, j > N_A \,, \end{array} \right. \tag{7.137}$$

$$|\Delta m^2_{N_A1}| \ll |\Delta m^2_{kj}| \quad \text{for} \quad \left\{ \begin{array}{c} k \leq N_A \quad \text{and} \quad j > N_A \\ \text{or} \\ k > N_A \quad \text{and} \quad j \leq N_A \,. \end{array} \right. \tag{7.138}$$

We are interested in the oscillations generated by $\Delta m^2_{N_A1}$. Because of the inequalities in eqn (7.137), we have

$$|\Delta m^2_{kj}| \simeq |\Delta m^2_{N_A1}|$$
$$\text{for} \quad (k \leq N_{A_1} \text{ and } N_{A_1} < j \leq N_A) \quad \text{or} \quad (N_{A_1} < k \leq N_A \text{ and } j \leq N_{A_1}) \,. \tag{7.139}$$

In an experiment which is sensitive to the oscillations generated by $\Delta m^2_{N_A1}$ we have

$$\frac{|\Delta m^2_{N_A1}|}{2} \left\langle \frac{L}{E} \right\rangle \sim \pi \,, \tag{7.140}$$

$$\frac{|\Delta m^2_{kj}|}{2}\left\langle\frac{L}{E}\right\rangle \ll \pi \quad \text{for} \quad \begin{cases} k,j \le N_{A_1} \\ \text{or} \\ N_{A_1} < k,j \le N_A \\ \text{or} \\ k,j > N_A\,, \end{cases} \tag{7.141}$$

$$\frac{|\Delta m^2_{kj}|}{2}\left\langle\frac{L}{E}\right\rangle \gg \pi \quad \text{for} \quad \begin{cases} k \le N_A \quad \text{and} \quad j > N_A \\ \text{or} \\ k > N_A \quad \text{and} \quad j \le N_A\,. \end{cases} \tag{7.142}$$

The inequalities in eqns (7.141) and (7.142) imply that

$$\left\langle\cos\left(\frac{\Delta m^2_{kj}L}{2E}\right)\right\rangle \simeq 1\,, \quad \left\langle\sin\left(\frac{\Delta m^2_{kj}L}{2E}\right)\right\rangle \ll 1 \quad \text{for} \quad \begin{cases} k,j \le N_{A_1} \\ \text{or} \\ N_{A_1} < k,j \le N_A \\ \text{or} \\ k,j > N_A\,, \end{cases} \tag{7.143}$$

$$\left\langle\cos\left(\frac{\Delta m^2_{kj}L}{2E}\right)\right\rangle \ll 1\,, \quad \left\langle\sin\left(\frac{\Delta m^2_{kj}L}{2E}\right)\right\rangle \ll 1 \quad \text{for} \quad \begin{cases} k \le N_A \,\text{and}\, j > N_A \\ \text{or} \\ k > N_A \,\text{and}\, j \le N_A\,. \end{cases} \tag{7.144}$$

Using these approximations, the effective probability obtained from eqn (7.37) is

$$\begin{aligned} P^{\text{eff}}_{\nu_\alpha\to\nu_\beta}(L,E) = \delta_{\alpha\beta} & \\ & - 2\left(\sum_{j\le N_{A_1}}\sum_{k=N_{A_1}+1}^{N_A} \Re\mathfrak{e}\left[U^*_{\alpha k}\,U_{\beta k}\,U_{\alpha j}\,U^*_{\beta j}\right]\right)\left[1-\cos\left(\frac{\Delta m^2_{N_A1}L}{2E}\right)\right] \\ & + 2\left(\sum_{j\le N_{A_1}}\sum_{k=N_{A_1}+1}^{N_A} \Im\mathfrak{m}\left[U^*_{\alpha k}\,U_{\beta k}\,U_{\alpha j}\,U^*_{\beta j}\right]\right)\sin\left(\frac{\Delta m^2_{N_A1}L}{2E}\right) \\ & - 2\sum_{j\le N_A}\sum_{k>N_A} \Re\mathfrak{e}\left[U^*_{\alpha k}\,U_{\beta k}\,U_{\alpha j}\,U^*_{\beta j}\right]\,. \end{aligned} \tag{7.145}$$

Let us consider first the survival probabilities. From eqn (7.145) for $\alpha = \beta$ we get

$$\begin{aligned} P^{\text{eff}}_{\nu_\alpha\to\nu_\alpha}(L,E) = 1 & - 4\left(\sum_{j\le N_{A_1}}|U_{\alpha j}|^2\right)\left(\sum_{k=N_{A_1}+1}^{N_A}|U_{\alpha k}|^2\right)\sin^2\left(\frac{\Delta m^2_{N_A1}L}{4E}\right) \\ & - 2\left(\sum_{k=1}^{N_A}|U_{\alpha k}|^2\right)\left(\sum_{k>N_A}|U_{\alpha k}|^2\right)\,, \end{aligned} \tag{7.146}$$

which can be written as

$$P^{\rm eff}_{\nu_\alpha\to\nu_\alpha}(L,E) = 1 - 4\left(\sum_{j\leq N_{A_1}}|U_{\alpha j}|^2\right)\left(\sum_{k=N_{A_1}+1}^{N_A}|U_{\alpha k}|^2\right)\sin^2\left(\frac{\Delta m^2_{N_A1}L}{4E}\right) - 2\left(\sum_{k>N_A}|U_{\alpha k}|^2\right)\left(1-\sum_{k>N_A}|U_{\alpha k}|^2\right), \quad (7.147)$$

Let us separate the contributions due to the mixing of ν_α with the massive neutrinos ν_k belonging to the group B from those belonging to the group A. This task can be accomplished by writing the survival probability in eqn (7.147) as

$$P^{\rm eff}_{\nu_\alpha\to\nu_\alpha}(L,E) = \left(1-\sum_{k>N_A}|U_{\alpha k}|^2\right)^2 P^{(N_A,1)}_{\nu_\alpha\to\nu_\alpha}(L,E) + \left(\sum_{k>N_A}|U_{\alpha k}|^2\right)^2, \quad (7.148)$$

with

$$P^{(N_A,1)}_{\nu_\alpha\to\nu_\alpha}(L,E) = 1 - 4\,\frac{\left(\sum_{k\leq N_{A_1}}|U_{\alpha k}|^2\right)\left(\sum_{k=N_{A_1}+1}^{N_A}|U_{\alpha k}|^2\right)}{\left(\sum_{k=1}^{N_A}|U_{\alpha k}|^2\right)^2}\sin^2\left(\frac{\Delta m^2_{N_A1}L}{4E}\right). \quad (7.149)$$

This is a two-neutrino-like survival probability that can be written as

$$P^{(N_A,1)}_{\nu_\alpha\to\nu_\alpha}(L,E) = 1 - \sin^2 2\vartheta^{\rm eff}_{\alpha\alpha}\,\sin^2\left(\frac{\Delta m^2_{N_A1}L}{4E}\right), \quad (7.150)$$

with effective squared-mass difference $\Delta m^2_{N_A1}$ and effective mixing angle $\vartheta^{\rm eff}_{\alpha\alpha}$ given by

$$\sin^2 2\vartheta^{\rm eff}_{\alpha\alpha} = 4\,\frac{\left(\sum_{k\leq N_{A_1}}|U_{\alpha k}|^2\right)\left(\sum_{k=N_{A_1}+1}^{N_A}|U_{\alpha k}|^2\right)}{\left(\sum_{k=1}^{N_A}|U_{\alpha k}|^2\right)^2}. \quad (7.151)$$

This definition of an effective mixing angle is consistent because

$$\frac{\left(\sum_{k\leq N_{A_1}}|U_{\alpha k}|^2\right)\left(\sum_{k=N_{A_1}+1}^{N_A}|U_{\alpha k}|^2\right)}{\left(\sum_{k=1}^{N_A}|U_{\alpha k}|^2\right)^2} = \frac{\sum_{k\leq N_{A_1}}|U_{\alpha k}|^2}{\sum_{k=1}^{N_A}|U_{\alpha k}|^2}\left(1-\frac{\sum_{k\leq N_{A_1}}|U_{\alpha k}|^2}{\sum_{k=1}^{N_A}|U_{\alpha k}|^2}\right) \quad (7.152)$$

reaches its maximum value 1/4 for $\sum_{k\leq N_{A_1}}|U_{\alpha k}|^2/\sum_{k=1}^{N_A}|U_{\alpha k}|^2 = 1/2$. There are two possible values of the effective mixing angles symmetric with respect to $\pi/4$, given by

$$\sin\vartheta^{\rm eff}_{\alpha\alpha} = \sqrt{\frac{\sum_{k\leq N_{A_1}}|U_{\alpha k}|^2}{\sum_{k=1}^{N_A}|U_{\alpha k}|^2}} \quad \text{or} \quad \sin\vartheta^{\rm eff}_{\alpha\alpha} = \sqrt{\frac{\sum_{k=N_{A_1}+1}^{N_A}|U_{\alpha k}|^2}{\sum_{k=1}^{N_A}|U_{\alpha k}|^2}}. \quad (7.153)$$

Equation (7.148) is rather meaningful, because it shows that the effective survival probability $P^{\rm eff}_{\nu_\alpha\to\nu_\alpha}(L,E)$ deviates from being two-neutrino-like because of the

mixing of ν_α with the massive neutrinos belonging to the group B, which contributes with a constant term and with a suppression factor of the two-neutrino-like survival probability $P^{(N_A,1)}_{\nu_\alpha\to\nu_\alpha}(L,E)$. Both effects depend only on the sum of the squared absolute values of the elements of the mixing matrix that connect ν_α with the massive neutrinos belonging to the group B.

The effective survival probability $P^{\text{eff}}_{\nu_\alpha\to\nu_\alpha}(L,E)$ represents a great simplification with respect to the general form of the survival probability, which depends on many parameters, whereas eqn (7.148) depends on only three parameters: $\Delta m^2_{N_A1}$, $\sin^2 2\vartheta^{\text{eff}}_{\alpha\alpha}$ and $\sum_{k>N_A}|U_{\alpha k}|^2$. This is very useful in the analysis of experimental data.

In the limit of zero or negligible mixing of ν_α with the massive neutrinos belonging to the group B, the present case becomes coincident with the case of dominance of one scale of squared-mass differences discussed in the previous section 7.7. Indeed, the effective survival probability in eqn (7.148) is reduced to the two-neutrino-like survival probability in eqn (7.150), which is analogous to in eqn (7.133) with the appropriate change of the mixing parameters. The definition in eqn (7.151) of effective mixing angle becomes analogous to that in eqn (7.134) because in this case $\sum_{k=1}^{N_A}|U_{\alpha k}|^2 = 1$.

Unfortunately, the calculation of the transition probabilities is more cumbersome. Taking into account that $\alpha \neq \beta$, the unitary relation in eqn (7.28) implies that

$$\sum_{j\leq N_A}\sum_{k>N_A} U^*_{\alpha k}\,U_{\beta k}\,U_{\alpha j}\,U^*_{\beta j} = -\left|\widetilde{\sum_k}\,U^*_{\alpha k}\,U_{\beta k}\right|^2 , \tag{7.154}$$

where the symbol $\widetilde{\sum}_k$ has the same meaning as in eqn (7.122). Moreover, we have

$$\begin{aligned}\sum_{j\leq N_{A_1}}\sum_{k=N_{A_1}+1}^{N_A} U^*_{\alpha k}\,U_{\beta k}\,U_{\alpha j}\,U^*_{\beta j} &= -\left|\sum_{k\leq N_{A_1}} U^*_{\alpha k}\,U_{\beta k}\right|^2 - \sum_{j\leq N_{A_1}}\sum_{k>N_A} U^*_{\alpha k}\,U_{\beta k}\,U_{\alpha j}\,U^*_{\beta j} \\ &= -\left|\sum_{k=N_{A_1}+1}^{N_A} U^*_{\alpha k}\,U_{\beta k}\right|^2 - \sum_{j=N_A+1}^{N}\sum_{k=N_{A_1}+1}^{N_A} U^*_{\alpha k}\,U_{\beta k}\,U_{\alpha j}\,U^*_{\beta j}\,.\end{aligned} \tag{7.155}$$

Choosing the first equality in eqn (7.155) and the second equality in eqn (7.122), the effective transition probabilities can be written as

$$\begin{aligned}P^{\text{eff}}_{\nu_\alpha\to\nu_\beta}(L,E) = 4&\left|\sum_{k\leq N_{A_1}} U^*_{\alpha k}\,U_{\beta k}\right|^2 \sin^2\left(\frac{\Delta m^2_{N_A1}L}{4E}\right) \\ &+ 4\left(\sum_{j\leq N_{A_1}}\sum_{k>N_A}\Re\mathfrak{e}\left[U^*_{\alpha k}\,U_{\beta k}\,U_{\alpha j}\,U^*_{\beta j}\right]\right)\sin^2\left(\frac{\Delta m^2_{N_A1}L}{4E}\right)\end{aligned}$$

$$+ 2 \left(\sum_{j \leq N_{A_1}} \sum_{k > N_A} \Im\mathfrak{m}\left[U^*_{\alpha k} \, U_{\beta k} \, U_{\alpha j} \, U^*_{\beta j} \right] \right) \sin\left(\frac{\Delta m^2_{N_A 1} L}{2E} \right)$$

$$+ 2 \left| \sum_{k > N_A} U^*_{\alpha k} \, U_{\beta k} \right|^2 . \qquad (7.156)$$

The last term, which is constant, depends on the mixing of ν_α and ν_β with the massive neutrinos belonging to the group B. The first term, which is oscillating, depends on the mixing of ν_α and ν_β with the massive neutrinos belonging to the group A. The other two oscillating terms depend on the mixing of ν_α and ν_β with both the massive neutrinos belonging to the groups A and B. Clearly, it is not possible to separate completely the contributions due to the mixing of ν_α and ν_β with the massive neutrinos belonging to the groups A and B and write the contribution due to the mixing of ν_α and ν_β with the massive neutrinos belonging to the groups A in terms of an effective two-neutrino-like transition probability, because a two-neutrino-like transition probability cannot account for the effect of the phases in the mixing matrix, which in general are present in eqn (7.156) if the mixing of ν_α and ν_β with the massive neutrinos belonging to the group B is not zero. Only if such mixing is zero is there no effect of the phases, because the present case becomes coincident with the case of dominance of one scale of squared-mass differences discussed in the previous section 7.7. Indeed, in this limit only the first term on the right-hand side of eqn (7.156) survives and one can see that it is analogous to eqn (7.124) with the appropriate change of the mixing parameters.

Nevertheless, one must realize that the effective transition probability $P^{\text{eff}}_{\nu_\alpha \to \nu_\beta}(L, E)$ represents a great simplification with respect to the general form of the transition probability, which depends on many parameters. Indeed, eqn (7.148) depends on only five parameters: $\Delta m^2_{N_A 1}$, $\left| \sum_{k \leq N_{A_1}} U^*_{\alpha k} \, U_{\beta k} \right|^2$, $\sum_{j \leq N_{A_1}} \sum_{k > N_A} \Re\mathfrak{e}\left[U^*_{\alpha k} \, U_{\beta k} \, U_{\alpha j} \, U^*_{\beta j} \right]$, $\sum_{j \leq N_{A_1}} \sum_{k > N_A} \Im\mathfrak{m}\left[U^*_{\alpha k} \, U_{\beta k} \, U_{\alpha j} \, U^*_{\beta j} \right]$, and $\left| \sum_{k > N_A} U^*_{\alpha k} \, U_{\beta k} \right|^2$. This is very useful in practice, because it simplifies considerably the analysis of experimental data.